SEISMIC PERFORMANCE INVESTIGATION

OF THE

HAYWARD BART ELEVATED SECTION

by

Wen S. Tseng, Ming S. Yang and Joseph Penzien

International Civil Engineering Consultants, Inc.
1995 University Avenue, Suite 119
Berkeley, California 94704

Data Utilization Report CSMIP/92-02

California Strong Motion Instrumentation Program

September 1992

This study was conducted at the International Civil Engineering Consultants and was supported by the Department of Conservation under Contract No. 1090-501.

California Department of Conservation
Division of Mines and Geology
Office of Strong Motion Studies
801 K Street, MS 13-35
Sacramento, California 95814-3531

DIVISION OF MINES AND GEOLOGY
JAMES F. DAVIS
STATE GEOLOGIST

DISCLAIMER

The content of this report was developed under Contract No. 1090-501 from the Strong Motion Instrumentation Program in the Division of Mines and Geology of the California Department of Conservation. This report has not been edited to the standards of a formal publication. Any opinions, findings, conclusions or recommendations contained in this report are those of the authors, and should not be interpreted as representing the official policies, either expressed or implied, of the State of California.

PREFACE

The California Strong Motion Instrumentation Program (CSMIP) in the Division of Mines and Geology of the California Department of Conservation promotes and facilitates the improvement of seismic codes through the Directed Research Project. The objective of the this project is to increase the understanding of earthquake strong ground shaking and its effects on structures through interpretation and analysis studies of CSMIP and other applicable strong motion data. The ultimate goal is to accelerate the process by which lessons learned from earthquake data are incorporated into seismic code provisions and seismic design practices.

The specific objectives of the CSMIP Directed Research Project are to:

1. Understand the spatial variation and magnitude dependence of earthquake strong ground motion.

2. Understand the effects of earthquake motions on the response of geologic formations, buildings and lifeline structures.

3. Expedite the incorporation of knowledge of earthquake shaking into revision of seismic codes and practices.

4. Increase awareness within the seismological and earthquake engineering community about the effective usage of strong motion data.

5. Improve instrumentation methods and data processing techniques to maximize the usefulness of SMIP data. Develop data representations to increase the usefulness and the applicability to design engineers.

This report is the second in a series of CSMIP data utilization reports designed to transfer recent research findings on strong-motion data to practicing seismic design professionals and earth scientists. CSMIP extends its appreciation to the members of the Strong Motion Instrumentation Advisory Committee and its subcommittees for their recommendations regarding the Directed Research Project.

Moh J. Huang
CSMIP Directed Research
Project Manager

Anthony F. Shakal
CSMIP Program Manager

ABSTRACT

This final report presents the results of a seismic performance investigation of the Hayward BART elevated section, instrumented by the California Division of Mines and Geology under its Strong Motion Instrumentation Program (CSMIP), using the acceleration time-histories recorded during the October 17, 1989 Loma Prieta earthquake. The recorded structural responses are correlated with corresponding theoretically-predicted responses. Adjustments of structural parameters and modelling concepts required to achieve satisfactory correlations are discussed, along with their implications to procedures of standard engineering practice. The results obtained in this study indicate that during the Loma Prieta earthquake, the maximum seismic demand in the pier-columns of this section of the BART elevated structures was at the level of about 50% of the full-yield capacities of the columns; that soil-structure interaction effects play a significant role in controlling the seismic response characteristics in the transverse direction; and that, due to the presence of the continuous rails which are rigidly fastened to the girders, the BART elevated structures are highly coupled in the longitudinal direction; therefore, the single-pier model used for design in this direction may be inappropriate, especially for those elevated sections which have large variations in pier-column heights. Due to the importance of including soil-structure interaction considerations in the seismic modelling for this type of structure, the studies conducted point out an urgent need of instrumentation that allows independent recordings of the foundation response motions at the pier-column bases. Recommendations are made toward

improving the arrangement of CSMIP strong-motion instruments at the Hayward BART site to fulfill this need.

ACKNOWLEDGEMENT

The contents of this report were developed under contract No. 1090-501 from the California Department of Conservation, Division of Mines and Geology, Strong Motion Instrumentation Program. However, those contents do not necessarily represent the policy of that agency nor endorsement by the State of California.

In addition to the funding received under the above-mentioned contract, secondary funding was provided by International Civil Engineering Consultants, Inc. Mr. Matt McDole and Mr. Mark Chu of Bay Area Rapid Transit (BART) District, and Mr. Matt Hsiao of Bay Area Transit Consultants, Inc. provided much valuable information on the structure investigated. These funding and information sources are gratefully acknowledged.

TABLE OF CONTENTS

I. INTRODUCTION

The design of the present Bay Area Rapid Transit (BART) system started in 1963 and continued over a number of years. The state-of-the-art in the analysis and design of earthquake-resistant transportation structures has improved significantly since that time. Observing the performances of such structures during past earthquakes has been a major factor in bringing about this improvement. Most notably is the San Fernando earthquake of February 9, 1971, during which many elevated freeway structures collapsed. Following this event, major changes were made to the earthquake code provisions leading to improved structures from a seismic performance point of view (Ref. 1). As evidence of this fact, no freeway structures of post-San Fernando design suffered damages during the Loma Prieta earthquake, while many of such structures of pre-San Fernando design were heavily damaged and/or collapsed.

While the BART aerial structures were undamaged during the Loma Prieta earthquake, that fact alone does not insure satisfactory performance under future moderate to maximum credible earthquake conditions. Considering that the CSMIP-instrumented section of the Hayward BART aerial structure experienced deck-level peak horizontal accelerations as high as 0.60g during the Loma Prieta earthquake, even though the peak free-field horizontal ground acceleration at the site was only about 0.16g, its performance under free-field ground motions of two to four times this intensity of shaking is of considerable concern. Fortunately, the CSMIP recordings of structural response at this site have made it possible to

develop realistic modelling of this structure, allowing not only an assessment of its performance during the Loma Prieta earthquake but an assessment of its expected performance during an earthquake of much higher intensity, say 0.70g peak ground acceleration (PGA).

The objective of this report is to correlate the CSMIP recorded motions of the Hayward BART aerial structure produced by the Loma Prieta earthquake with predicted motions generated through mathematical modelling and analysis; thus, allowing improvements to be made in the current state-of-the-art of assessing the performance of such structures under seismic conditions.

II. DESCRIPTION OF STRUCTURE INVESTIGATED

The structure investigated under this study is a three-span nearly-straight section of the BART elevated system located immediately to the north of the Hayward BART Station. Fig. 1 shows the location of this structure and its relative position to the Hayward BART Station, while Fig. 2 shows its structural configuration and gross dimensions. As seen in the latter figure, the structure consists of 3 simply-supported twin box-girders constructed of prestressed concrete, which are supported on four single-column piers designated as P132, P133, P134, and P135.

The reinforced concrete single-column piers have a hexagonal cross-section with a 5-foot dimension between opposite faces and they are reinforced with two rings of #18 Grade 40 reinforcing bars, as shown in Fig. 3. Each column of piers P132, P133, and P135 has 28-#18 bars in its outer ring which run the full height from the top of the pier beam to the bottom of the column footing, and has 16-#18 bars in its inner ring which are cut at various heights; thus, for each column, a total of 44-#18 bars are present at its base. The column at pier P134 has 24 full-length #18 bars in its outer ring and 12-#18 bars cut at various heights in its inner ring; thus, it has a total of 36-#18 bars present at its base. All columns are provided with #5 spiral bars running at 3-inch pitch covering almost the full height of column.

Each pier-column of P132 and P133 is supported on a 16′ × 16′ square footing

5.5′ deep, which is, in turn, supported by 18 one-foot-diameter reinforced concrete piles, each having a capacity rating of 60 tons. Piers P134 and P135 are supported on a 15′ × 15′ square footing, 5.5′ deep, and on 16 and 18 piles, respectively, of the same capacity rating. Except for the vertical piles located along the horizontal axes of symmetry of the footing, all others are battered with a slope of 8:1 for the inner piles and 4:1 for the outer piles. All piles were driven into the soils to depths of 40 to 50 feet below the bottoms of the pier footings. The soil condition at the site, as indicated by the soil boring-logs for Bore Holes Nos. 50, 51, and 52 located near the site, consists of layers of sandy clay and silty sand. A site soil-profile and the foundation configurations of all four piers, P132 through P135, are schematically shown in Fig. 4. The water table at the site is located about 60 feet below ground surface.

Each prestressed-concrete box-girder is hinged at its north end to its corresponding pier-beam support through two vertical concrete-filled 5-inch-diameter steel pipes and it rests on a bearing support at its south end allowing freedom of movement longitudinally relative to the support. Freedom of relative movement transversely is prevented, however, since the south end of each girder is hinged to the north end of the adjacent girder. All hinges of the girders have a 1-inch gap, tight-fitted with a non-laminated elastomeric material and the girders themselves are supported on the tops of pier beams through two 15" × 12" × 1" elastomeric pads at each end of each girder. Thus, even for small relative displacements (<<1 inch), the stiffnesses of the elastomeric pipe-hinge fillers and bearing pads play a role in controlling the girder vibration frequencies.

The details of a girder support on a pier beam are shown schematically in Fig. 5.

The BART train rails are fastened rigidly to the prestressed-concrete girders at 3-foot intervals longitudinally by bolts embedded into the girder which anchor the rail-fastener assemblies. Thus, even though the girders are simply supported between adjacent piers, stiffness coupling across the girder joints between spans exists due to the stiffnesses of the continuous rails which are rigidly fastened to the girders. Such coupling is very significant in the longitudinal direction due to the high axial stiffness of the rails, but is not too significant in the transverse direction. As will be discussed later, the high stiffness coupling in the longitudinal direction did indeed play a major role in the seismic response behavior as recorded by the CSMIP instruments during the Loma Prieta earthquake.

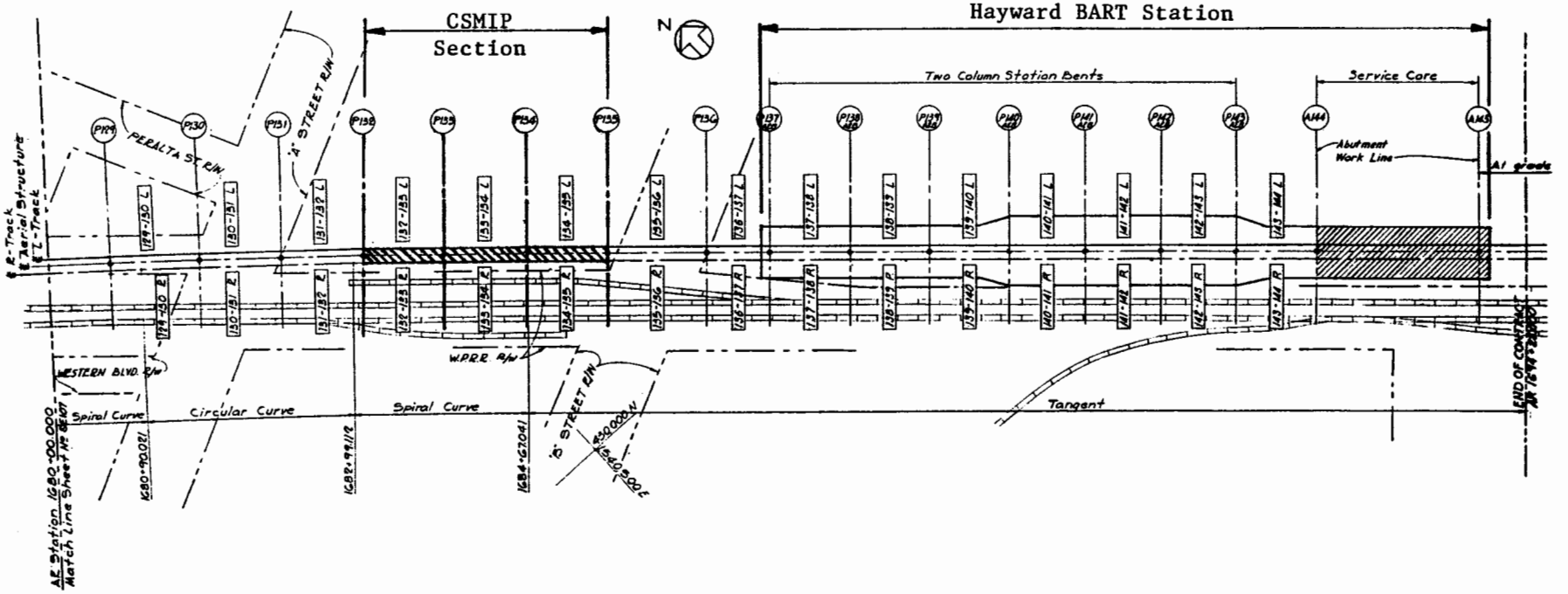

Figure 1 Location of the CSMIP-Instrumented BART Elevated Structure Relative to Hayward BART Station

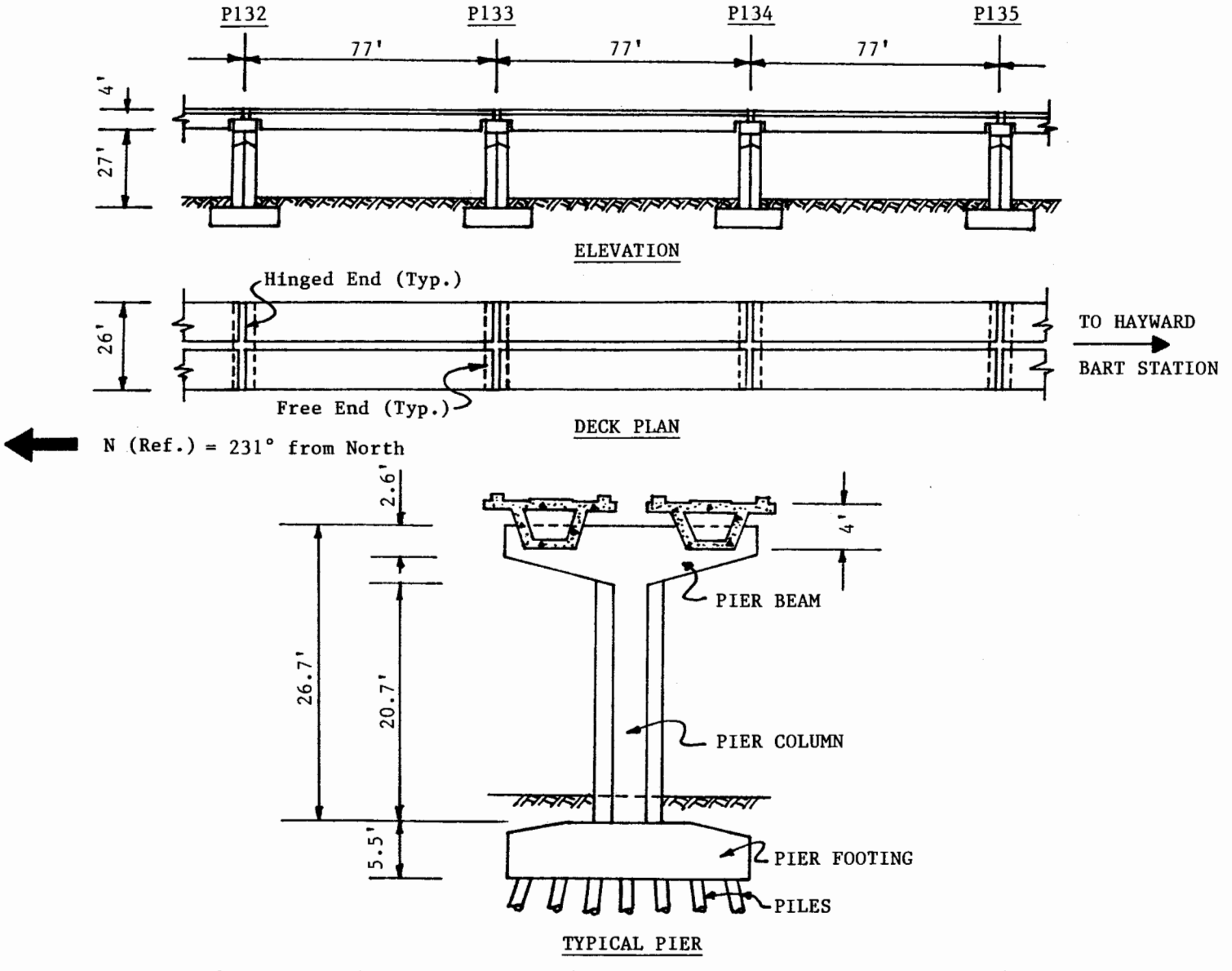

Figure 2 Structural Configuration and Dimensions of the CSMIP-Instrumented Section

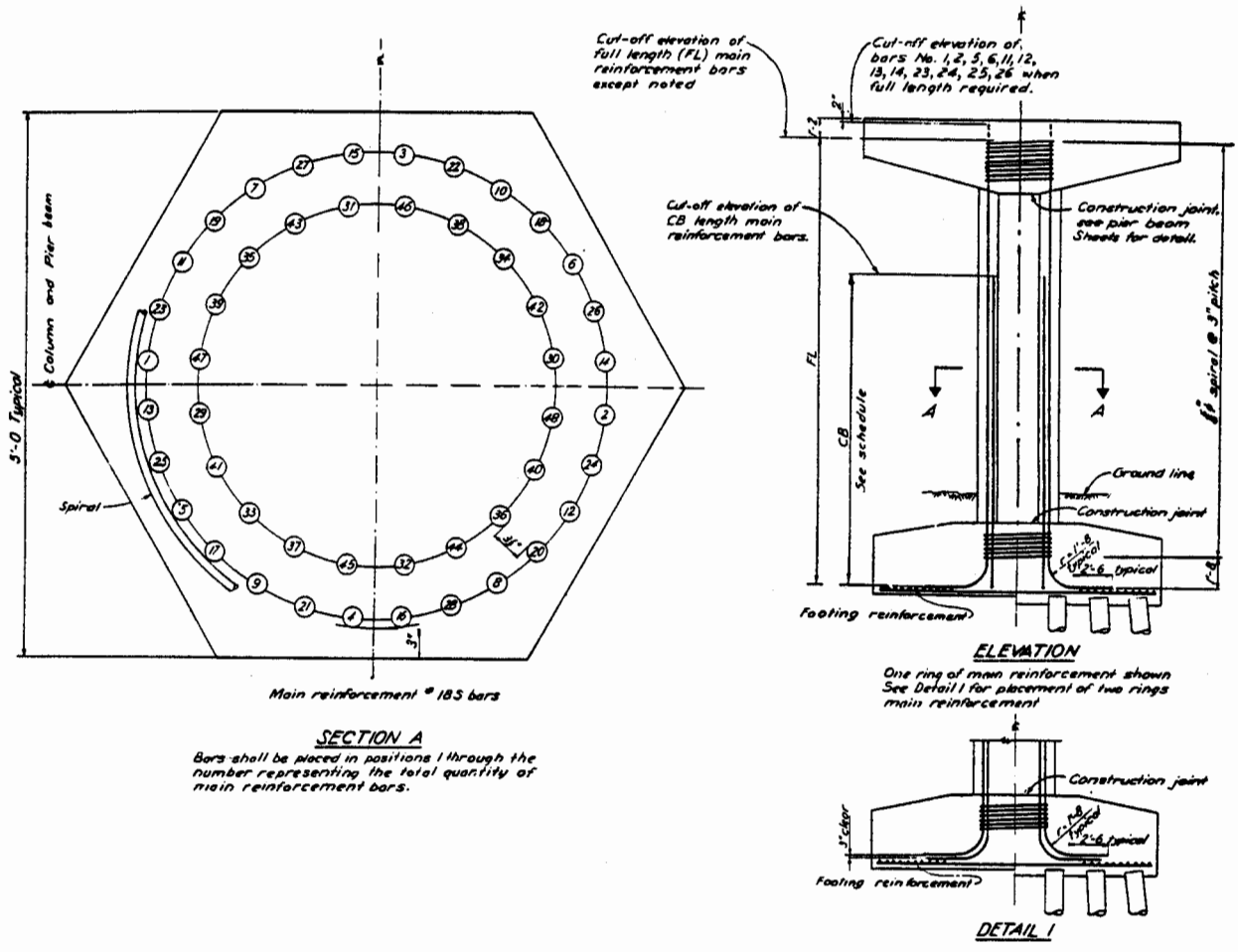

Figure 3 Pier Column Cross-Section and Reinforcing Details

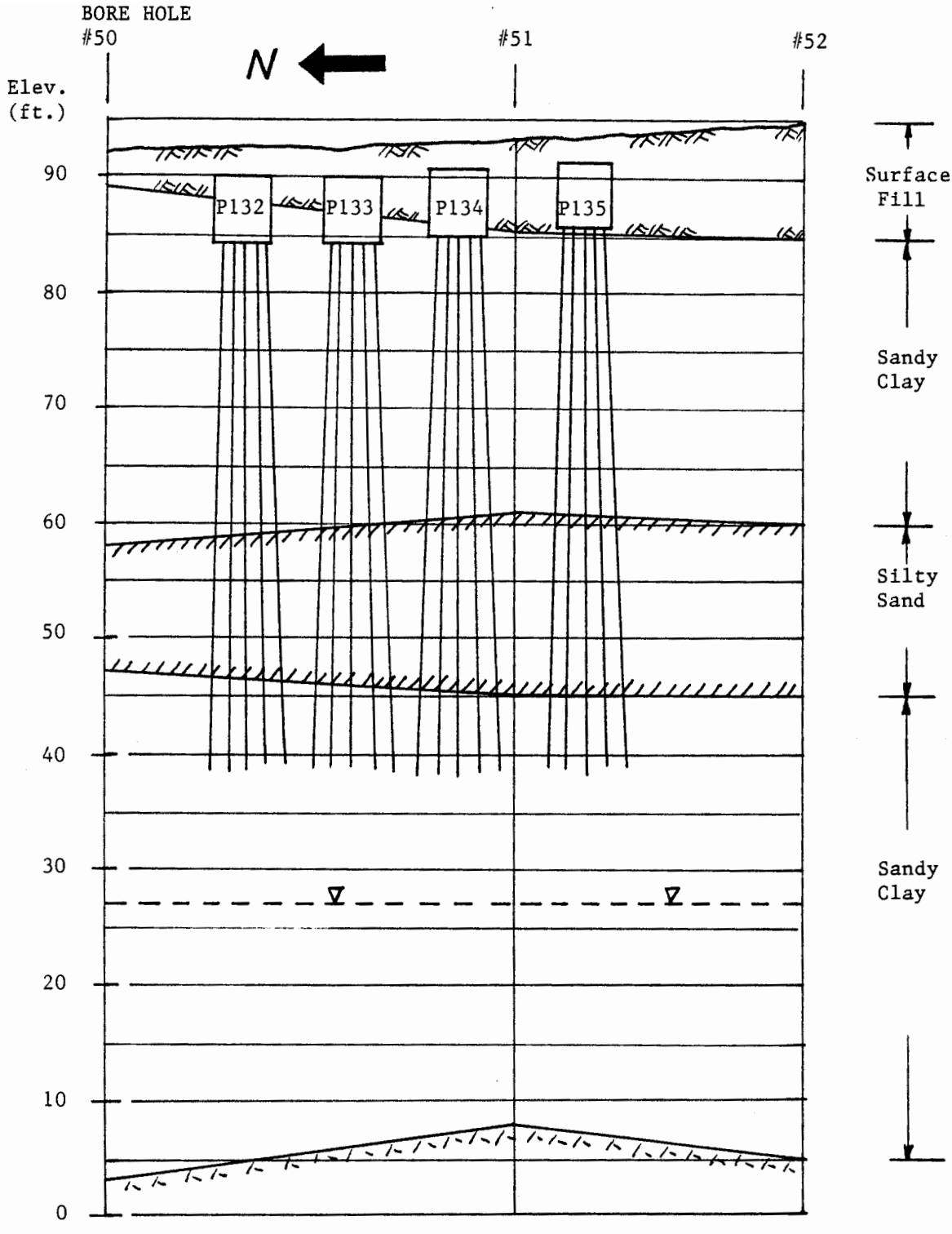

Figure 4 Site Soil Profile and Pile-Supported Foundation Configuration

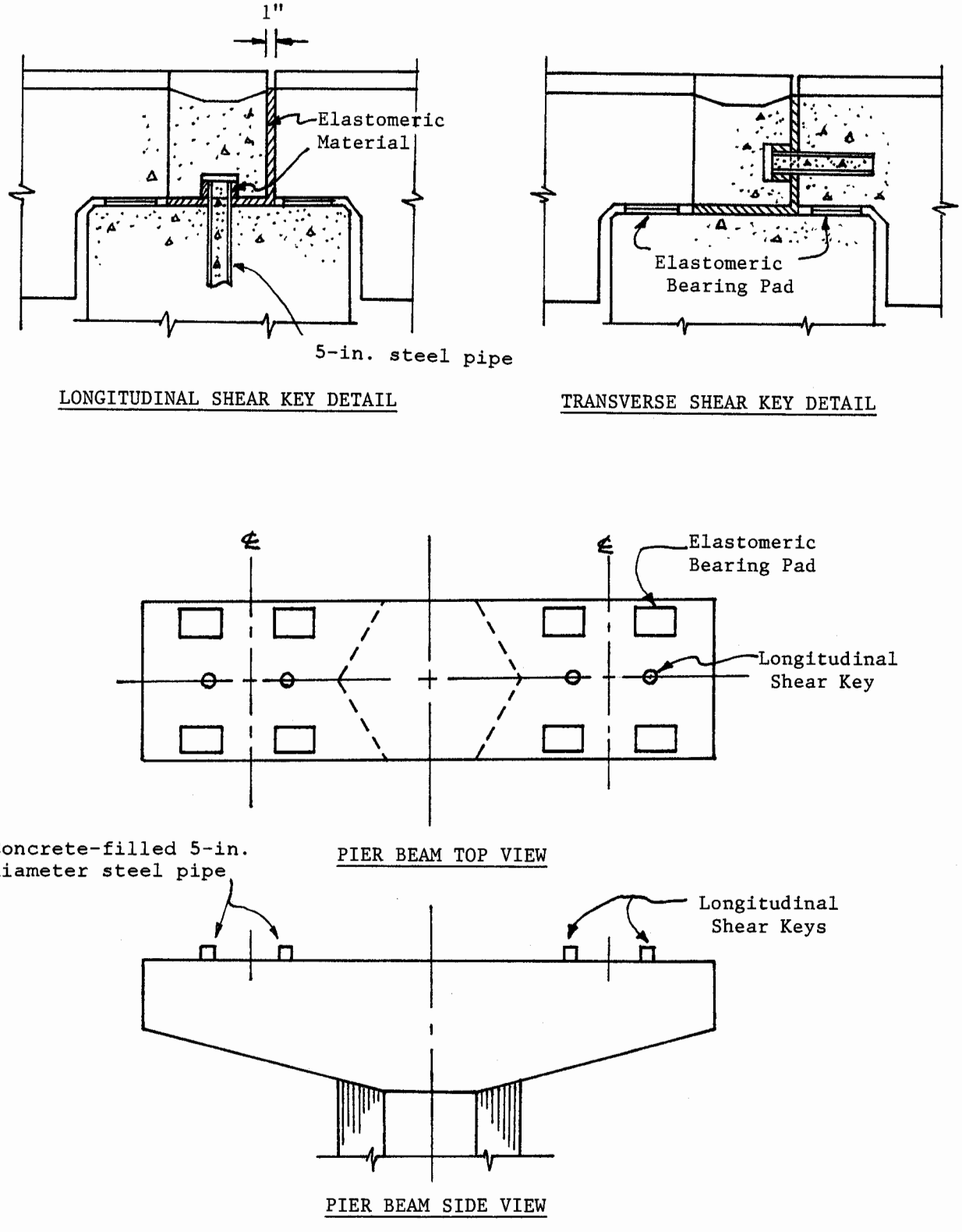

Figure 5 Details of Girder Joints and Girder-to-Pier-Beam Supports

III. DESCRIPTION OF INSTRUMENTATION AND DATA COLLECTED DURING LOMA PRIETA EARTHQUAKE

The CSMIP instrumentation of the structure under investigation consists of 18 strong-motion acceleration sensors installed both on the structure and in the free-field. These sensors will be designated herein as Channel Nos. 1 through 8 and 10 through 19 (Channel No. 9 was not installed). The locations and directions of sensors are shown in Fig. 6. As indicated in this figure, triaxial sets and individual sensors were installed at the following locations: (1) one set (Nos. 17, 18, and 19) in the free-field of a parking lot about 450 feet west and 640 feet south of the BART Station, (2) one set (Nos. 1, 2, and 13) at the base of pier P132, (3) one set (Nos. 14, 15, and 16) at the base of pier P135, (4) four individuals sensors (Nos. 5, 6, 7, and 8) at the undersides of the girder decks for measuring the longitudinal motions of the girders, (5) two individual sensors (Nos. 10 and 11) to measure transverse motions on the girder spanning between piers P132 and P133, (6) two individual sensors (Nos. 3 and 12) at the center of the pier beam of P132 to measure the longitudinal and transverse motions, respectively, and (7) one individual sensor (No. 4) at the east edge of the pier beam of P132 to measure longitudinal motion.

During the October 17, 1989 Loma Prieta earthquake, accelerograms were recorded by all 18 sensors. These accelerograms are shown as time-history plots in Fig. 7. The free-field recordings show that during the earthquake, the site region experienced ground-surface peak-accelerations of 0.16g horizontally and

0.08g vertically. The peak accelerations experienced at the girder deck level ranged from 0.39g to 0.60g in the transverse direction and from 0.21g to 0.26g in the longitudinal direction.

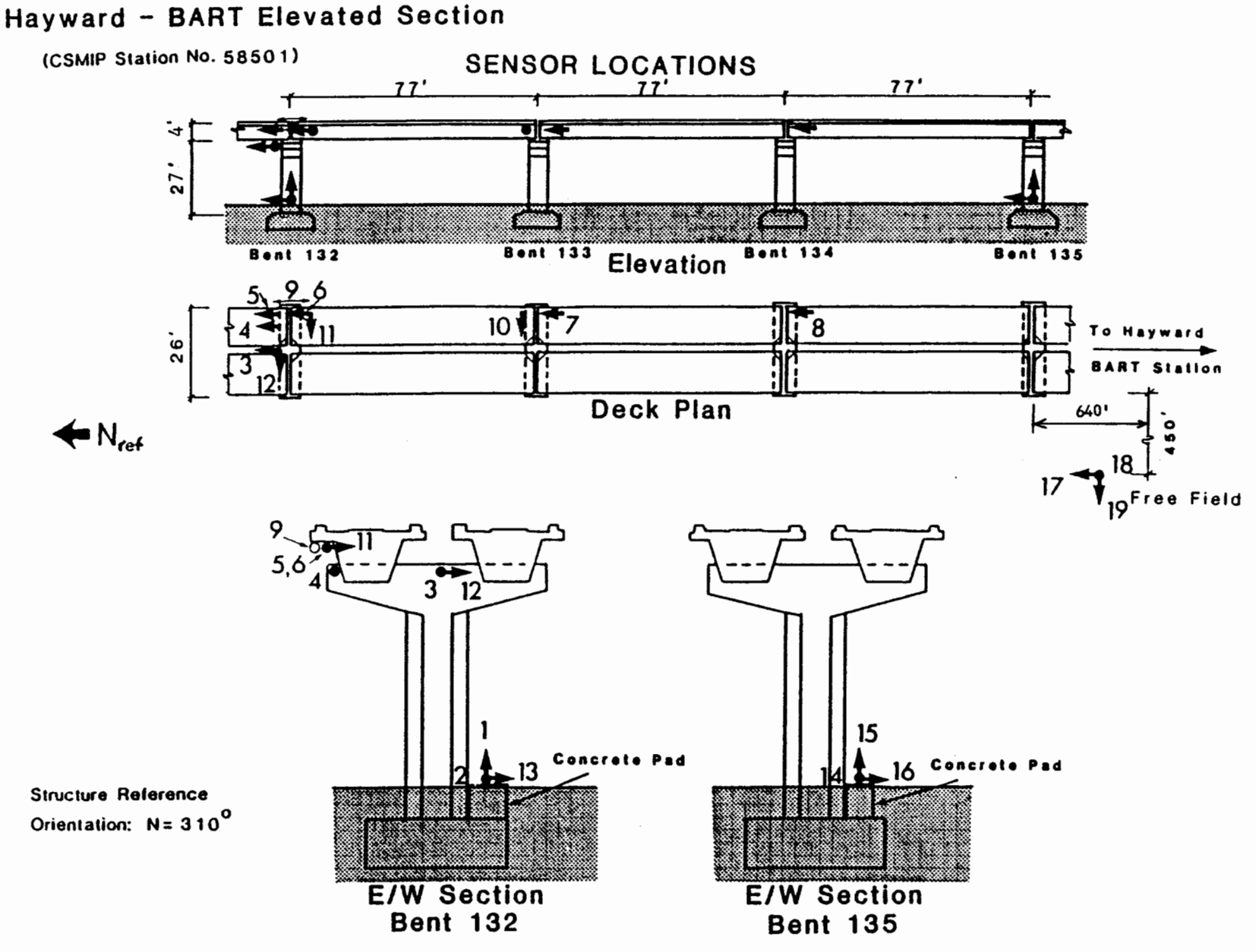

Figure 6 Structure Configuration of Hayward-BART Elevated Section and Sensor Locations

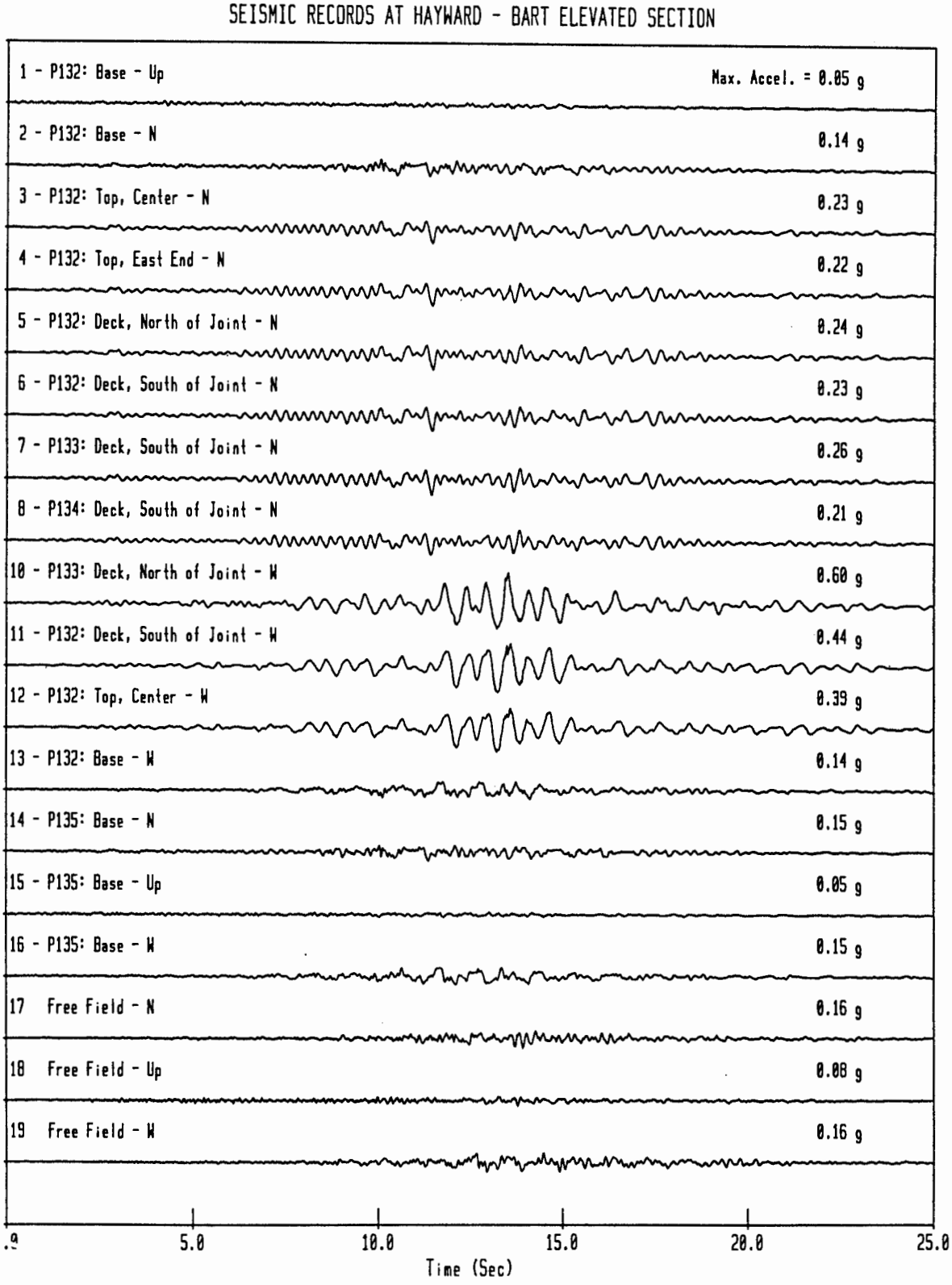

Figure 7 Accelerograms Recorded During the Loma Prieta Earthquake of 1989

IV. ANALYSIS OF RECORDED DATA AND OBSERVATIONS

The acceleration time-history data collected from the Loma Prieta earthquake shown in Fig. 7 have been analyzed extensively in this study in an attempt to understand the seismic response behavior of this structure during the earthquake. In general, the data analyses performed consisted of the following:

(1) Acceleration response spectra for 2% damping ratio (ξ = 0.02) were computed from the recorded acceleration time-history data. These computed spectra serve as an indication of the significant frequency contents in the motions from which the frequency ranges producing significant structural response amplifications can be identified. These spectra also serve as the bases with which the corresponding spectra obtained from the analytically-predicted motions have been compared to given an indication of degrees of correlation achieved.

(2) Fourier spectra of the acceleration time-histories recorded on the structure and in the free-field were computed and the transfer functions (complex Fourier spectrum ratios as functions of frequencies) between the structural response motions and the free-field motions were computed. These transfer functions reflect the dynamic response characteristics of the complete structure/foundation system under the excitation of the free-field input motions. The significant system frequencies and associated damping values were then determined from these transfer functions.

(3) The recorded acceleration time-histories were doubly integrated to give displacement time-histories from which selected relative displacement time-histories of interest, e.g., the relative displacement across a joint or girder support, were obtained.

(4) Cross-correlation functions between pairs of selected recorded motions were computed from which the apparent phase lags between these pairs of motions were determined.

From the results of the data analyses described above, significant features of the seismic response of the structure during the earthquake were observed and deduced. These are summarized in the following:

Free-Field Motions

The 2%-damped acceleration response spectra for the free-field recorded motions (Sensors 17, 18, and 19) were calculated and the results are shown in Fig. 8. Although the peak acceleration values recorded (0.16g) were about the same for the NS and EW directions, the EW motion, which is in the transverse direction of the structure, contains significant components of motion in a narrow frequency range near 1 Hz; whereas, the components of motion in this same frequency range are nearly absent in the NS longitudinal direction of the structure. Both horizontal motions contain significant components of motion in the frequency range of 4 to 10 Hz. The vertical component of motion has a

response spectral shape which closely resembles that of the NS motion, but its spectral amplitudes are about one-half of those representing the NS motion in the frequency range of 0.3 to 25 Hz. As will be shown later, the significant content of motion near 1 Hz for the EW motion has a significant effect on the transverse response of the structure.

Longitudinal Structural Response at the Deck Level

The longitudinal structural response motions at the deck level were recorded at 6 sensor locations, namely, those of Sensors 3, 4, 5, 6, 7, and 8 referred to in Fig. 6. Sensor locations 5, 6, 7, and 8 are on the girder, while those of Sensors 3 and 4 are on the pier beam. The recorded acceleration-response time-histories at all of these sensor locations are re-plotted together in Fig. 9 along with their 2%-damped acceleration response spectra. Examining the time-histories and spectra shown, one can observe that the longitudinal responses at all sensor locations along the 3-span length are almost identical, indicating that, even though joints are present, the girders are strongly coupled longitudinally by the rails; thus, they behave essentially as a unit in this direction with almost no relative motions taking place across the joints.

To examine the amount of relative motion across the girder joint on top of P132, two displacement time-histories were computed by CSMIP using the acceleration time-histories of Sensors 5 and 6, shown in Fig. 10. Subtracting one displacement time-history from the other gives the relative displacement

time-history shown in Fig. 10. It is recognized that an unknown amount of noise is present in this time-history. It is believed, however, that a significant portion of the maximum relative displacement equal to about 2 mm (0.08 inch) is real. Regardless of the uncertainty with regard to amount of noise present, the maximum relative displacement appears to be definitely less than 10% of the joint gap equal to 1 inch.

Because of the constraint provided by the rails, which run continuously across the girder-to-girder joint with fasteners connecting them to the girder on both sides at intervals of 36 inches, the girder ends on both sides of the joint move essentially the same in the longitudinal direction. If the joint gap did change by the amount indicated above, some slippage and/or deformation must have taken place in the adjacent fasteners.

To examine the longitudinal relative motion between the girder and the pier beam on top of P132, the integrated displacement time-histories of Sensors 4 and 5 provided by CSMIP and the corresponding relative displacement time-history computed from them are shown in Fig. 11. Even though some unknown amount of noise is present in this relative displacement time-history which represents shear deformation in the elastomeric bearing pad, its real maximum value appears to be about 2 mm (0.08 inch), which is relatively small considering that the girder at this end is free longitudinally..

The relative displacement time-histories in Figs. 10 and 11 appear to show

higher frequency contents than do the pairs of displacement time-histories from which they were derived. This is not the case, however, as the higher frequencies shown for the relative displacement time-histories are also present in the displacement time-histories. Visually, they are not apparent as the displacement time-histories are plotted to a scale which differs by a factor of 10 from that of the relative displacement time-histories. The significant difference is that the lower frequencies in the displacement time-histories are closely in phase with each other so that they get cancelled out when one displacement time-history is subtracted from the other. On the other hand, the higher frequencies in the displacement time-histories have large phase differences so that they do not get cancelled out when one displacement time-history is subtracted from the other.

Transverse Structural Response at the Deck Level

The transverse structural response motions at the deck level were recorded at 3 locations, namely, at the locations of Sensors 10, 11, and 12 as shown in Fig. 6. Sensors 10 and 11 are on the two ends of one girder spanning piers P132 and P133, whereas Sensor 12 is located at the top center of pier beam P132. The acceleration time-histories recorded and the 2%-damped response spectra computed from them are shown in Fig. 12. As seen in this figure, the recorded acceleration time-histories and their corresponding response spectra at the three locations show close resemblances; however, their amplitudes show some variations. This indicates that, transversely, the girder and the pier beam

basically responded as a unit with very little relative motion across the elastomeric bearing pads.

To examine in more detail the relative motion across the bearing pad, the integrated displacement time-histories at Sensors 11 and 12 and the relative displacement calculated from them are shown in Fig. 13. As seen, the relative displacement is in-phase with both individual displacements which are themselves in-phase with each other, indicating that the girder and the pier beam basically respond together. The maximum relative displacement shown in Fig. 13 is about 5.5 mm (0.216 inch). Using this amount of maximum relative displacement and the transverse inertia force of the girder tributary to pier P132, the apparent shear modulus of the elastomeric bearing pads, calculated taking into account the stiffnesses of elastomeric fillers around the hinges, is in the range of 500 to 600 psi which is about 4 to 5 times higher than the 120 to 155 psi given in the AASHTO code. In this estimate, the contribution to the maximum relative displacement due to the rotation of the pier beam is ignored. If this contribution is taken into account, the apparent shear modulus of the bearing pads would be even higher than the estimated values given above.

Longitudinal Structural Response Behavior at P132

Pier 132 has been instrumented with the largest number of sensors. There are 4 sensors measuring response of the pier in the longitudinal direction. Referring to Fig. 6, Sensors 3 and 4 measure responses of the pier beam at the

center and the east end, respectively; whereas Sensor 2 measures response at the pier base. Sensor 6, which is located on the end of the girder hinged to P132, measures the response of the girder. Comparing the recorded acceleration time-histories at sensor locations 3 and 4, shown in Fig. 7, and their integrated displacement time-histories shown in Fig. 14, one observes that the displacement responses at these two locations are very similar. The time-history of relative displacement between these locations is also shown in Fig. 14. The maximum relative displacement equal to about 1.5 mm (0.6 inch) corresponds to a pier beam rotation about the vertical axis equal to 0.00045 rads (0.026 degrees). This rotation corresponds to the total twist of the supporting single-column pier over its height of 27 feet. The corresponding maximum shear stress in the pier due to this twist, assuming no foundation rotation, is less than 50 psi.

To assess the longitudinal response behavior of P132, the 2%-damped acceleration response spectra computed for the motions recorded by Sensors 2 (base), 3 (pier beam center), 6 (girder deck level) and 17 (free-field) are shown in Fig. 15. The transfer function amplitudes computed between the structural response motions (measured by Sensors 2, 3, and 6) and the free-field motion (measured by Sensor 17) are also shown in this figure. As indicated by the transfer function amplitude plots and by the response spectrum plots, the structure system at P132 has a major structural amplification peak at the frequency of 3.5 Hz and minor peak at about 2.1 Hz. Minor peaks are also observed for the deck response at frequencies near 1.0 and 10.5 Hz. Using the half-power bandwidth method, the modal damping of the structural system for the

major response mode at 3.5 Hz is estimated to about 4%. By examining the transfer function amplitude-plot for the response at the pier base (Sensor 2), one can observe that a significant soil-structure interaction (SSI) effect was present during the earthquake.

Transverse Structural Response Behavior at P132

As shown in Fig. 6, three sensors measure structural response in the transverse direction, namely, Sensors 11 (deck level), 12 (pier beam center), and 13 (pier base). The 2%-damped acceleration response spectra computed for these recorded motions, along with that for the free-field motion in the EW direction (Sensor 19) are shown in Fig. 16 where they can be compared. Also shown in this figure are the transfer function amplitudes computed for the response motions relative to the free-field motion at Sensor 19. As indicated by these plots, the structure system at P132 in the transverse direction has major structural response peak at the frequency of 1.8 Hz and a minor response peak at 3.6 Hz. Again using the half-power bandwidth method, the modal damping of the system of the major response mode at 1.8 Hz is estimated to be about 3.6%. From the transfer function amplitude plot representing response motion at the pier base, one again observes that a significant SSI effect has taken place during the earthquake.

Structural Responses at the Bases of P132 and P135

Two sets of triaxial sensors were installed at the bases of piers P132 and P135 which are separated by a distance of 231 feet (70.4 m). By examining the recorded motions at these two locations, one can deduce the direction of seismic wave propagation during the event. The integrated displacement time-histories of the measured longitudinal motions (Sensors 2 and 14) are plotted in Fig. 17. As shown, the displacement time-histories at these two locations are very similar with the motion at P132 lagging behind that at P135 by a small amount, indicating that the seismic waves propagated in the general direction from South to North which is consistent with the relative location of the epicenter to the site. To estimate the time lag, the cross-correlation function between these two motions was computed as also shown in Fig. 17. Based on this results, the time lag for the longitudinal motions is estimated to be about 0.03 second. Thus, the apparent wave propagation velocity for the longitudinal component of motion in the longitudinal direction of the structure is estimated to be about 2.4 km/sec. Similarly, the integrated displacement time-histories of the measured transverse motions (Sensors 13 and 16) along with their cross-correlation functions are shown in Fig. 18. From the cross-correlation result shown in this figure, the time lag for the transverse motions is estimated to be about 0.07 second. Thus, the apparent wave propagation velocity for the transverse component of motion in the longitudinal direction of the structure is estimated to be about 1.0 km/sec.

To examine the seismic response characteristics of the pier bases of P132

and P135, the 2%-damped acceleration response spectra for the recorded NS and EW motions were computed and they are compared with the 2%-damped response spectra of the recorded free-field motions in the corresponding directions in Figs. 19 and 20, respectively. The transfer function amplitudes computed for the pier base response motions relative to the free-field motions are also shown in these figures. As shown in these figures, the spectra of pier base motions of P132 and P135 deviate significantly from those for the free-field motions and the computed transfer function amplitudes deviate significantly from unity, indicating that significant soil-structure interaction effects have taken place during the event.

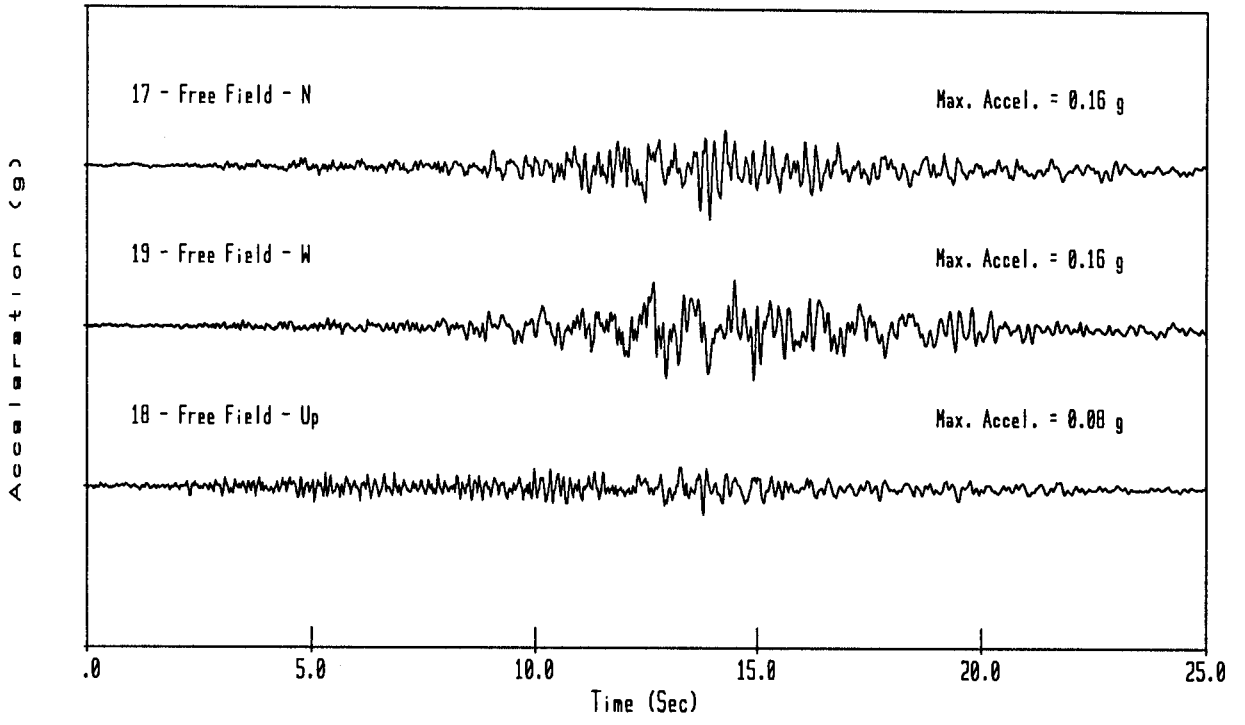

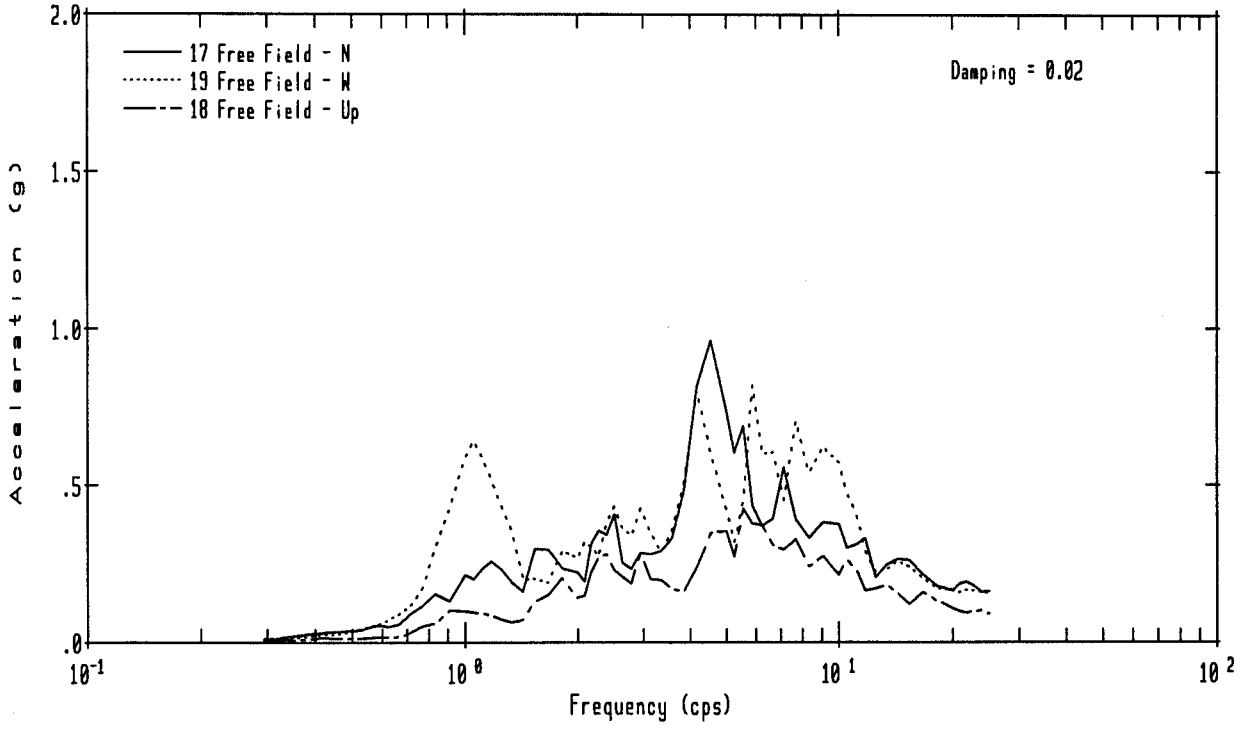

Figure 8 **Free-Field Recorded Accelerograms and Acceleration Response Spectra**

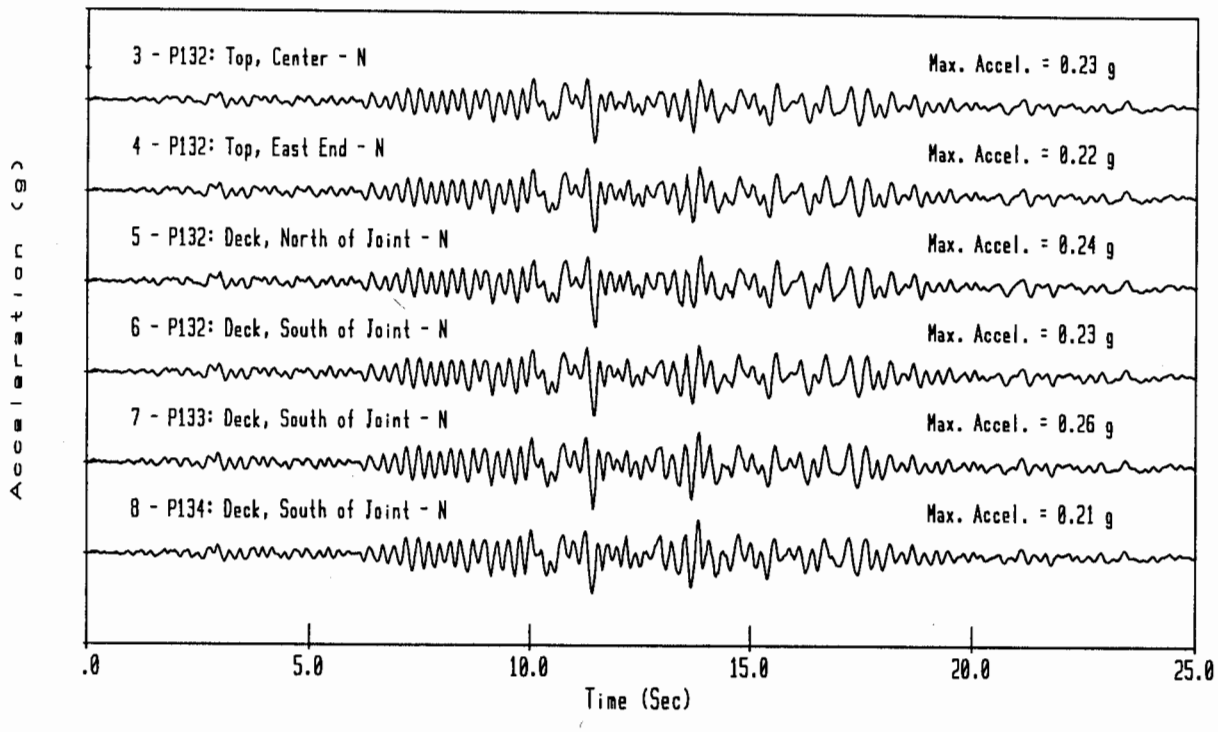

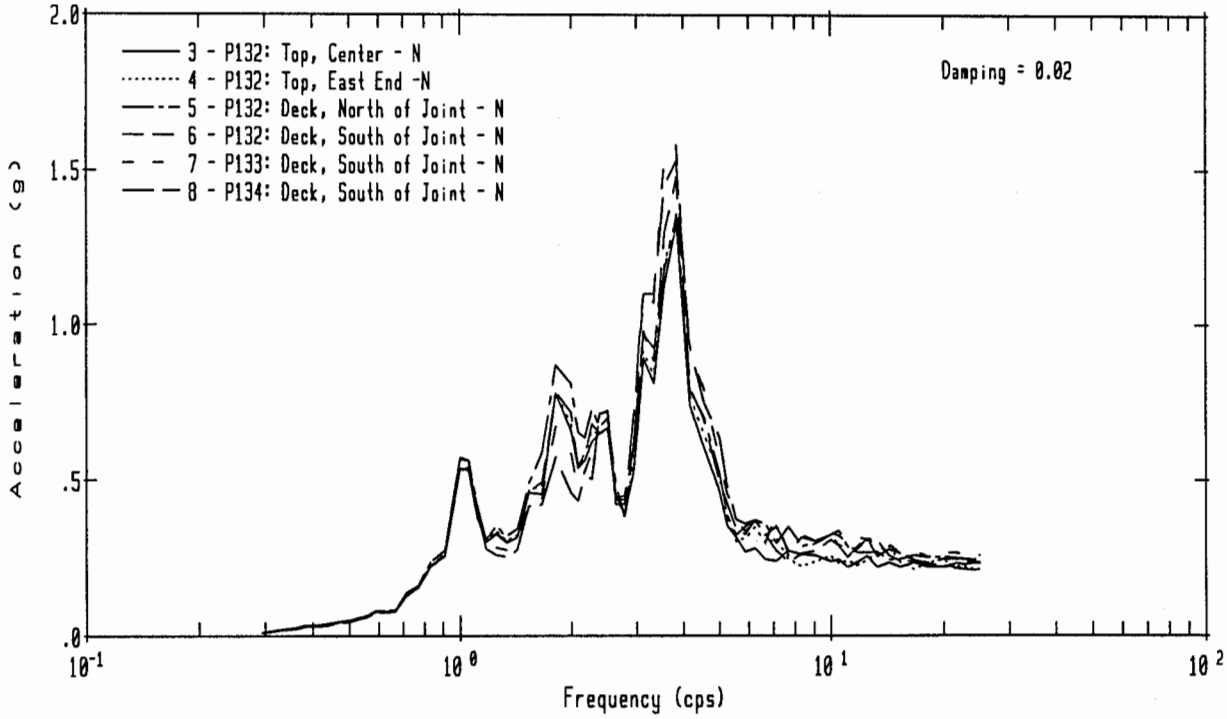

Figure 9 Recorded Longitudinal Acceleration Time-Histories and Their Computed 2%-Damped Acceleration Response Spectra at the Girder Deck Level

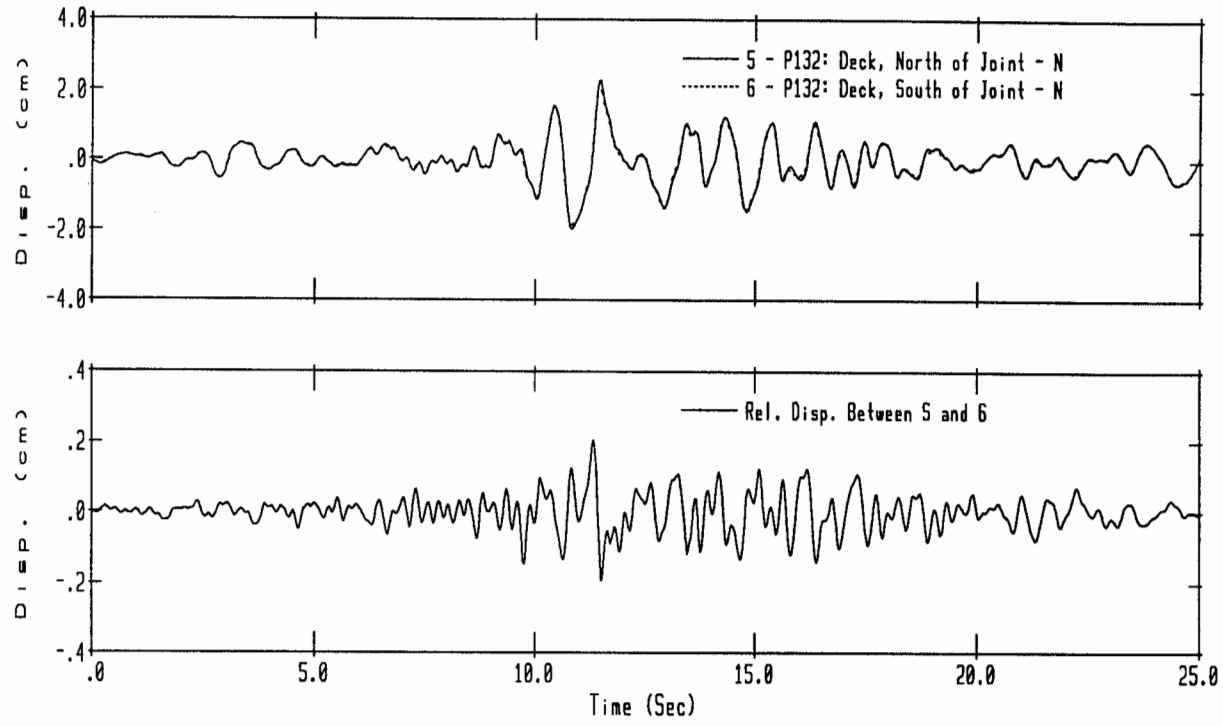

Figure 10 Comparison of Integrated Displacement Time-Histories at Sensors 5 and 6 and the Relative Displacement Time-History Computed from Them

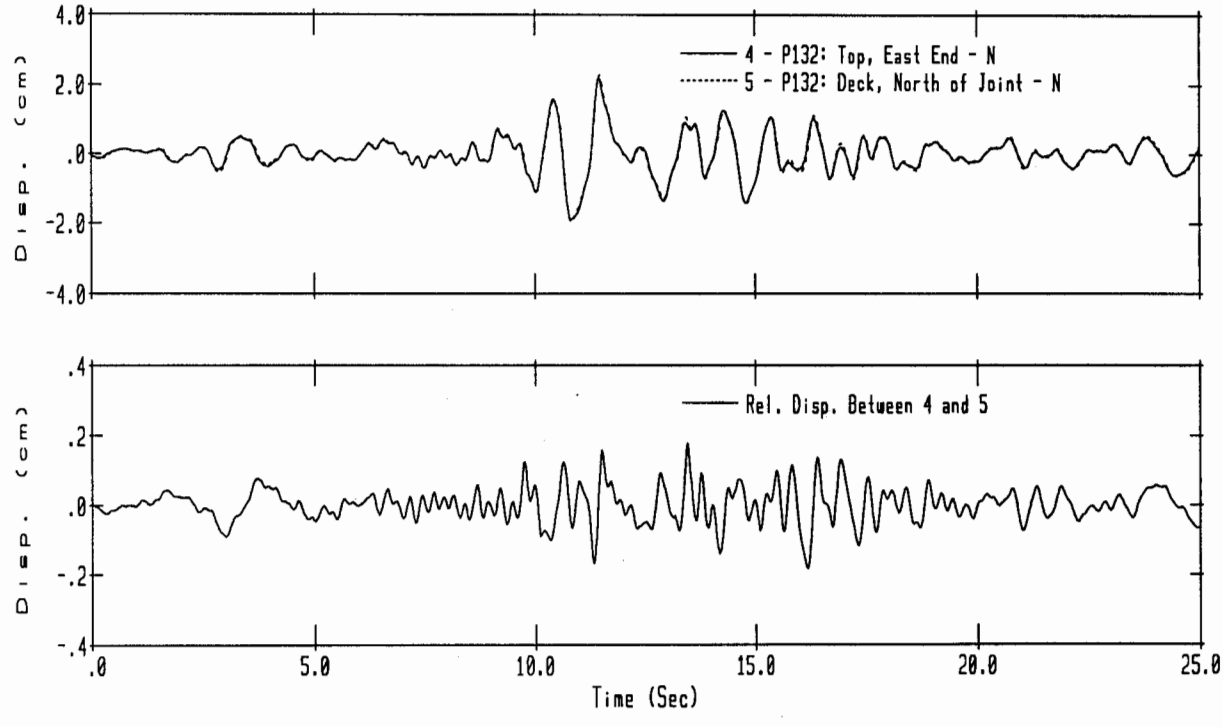

Figure 11 Comparison of Integrated Displacement Time-Histories at Sensors 4 and 5 and the Relative Displacement Time-History Computed from Them

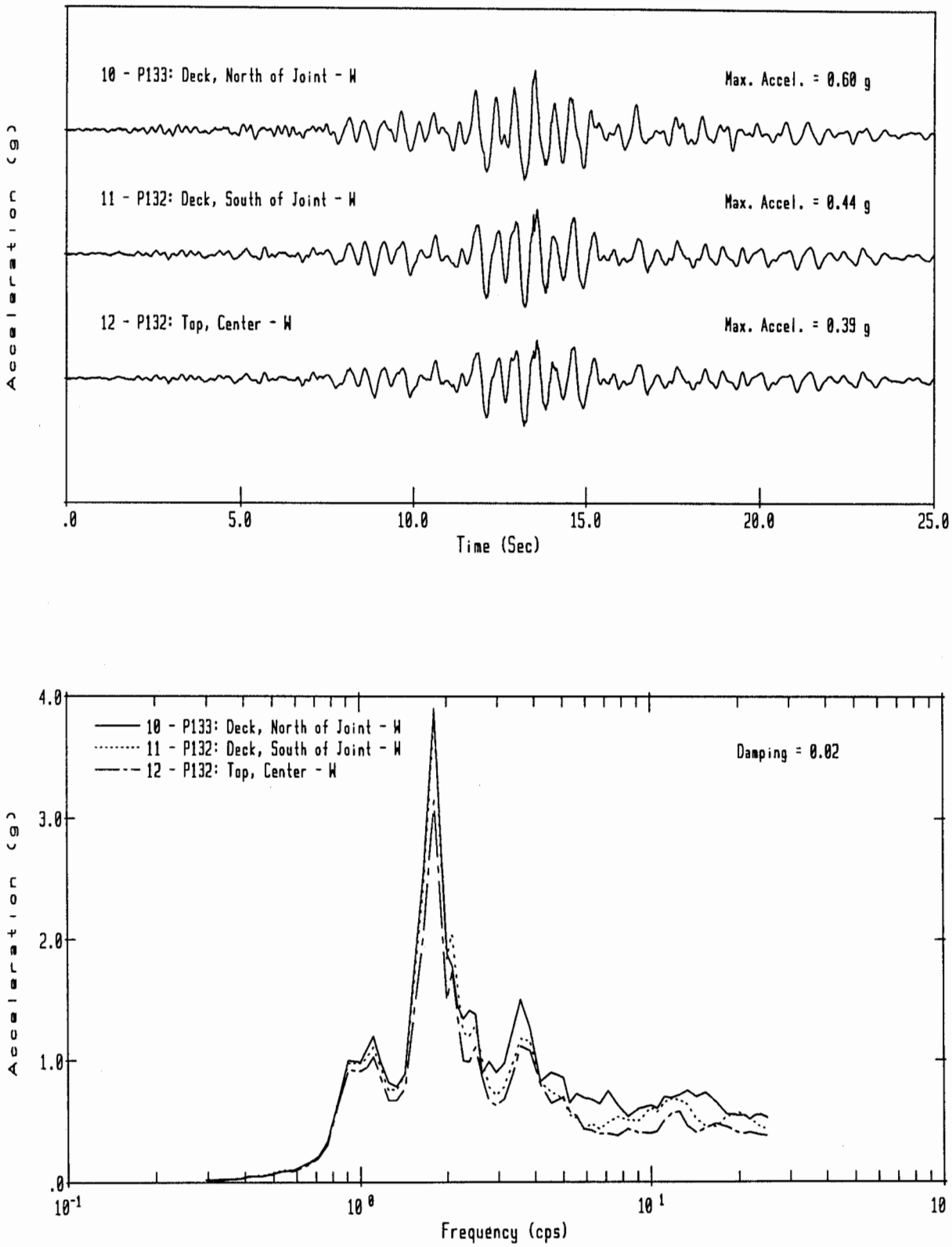

Figure 12 Recorded Transverse Acceleration Time-Histories and Their Computed 2% Damped Acceleration Response Spectra at the Girder Deck Level

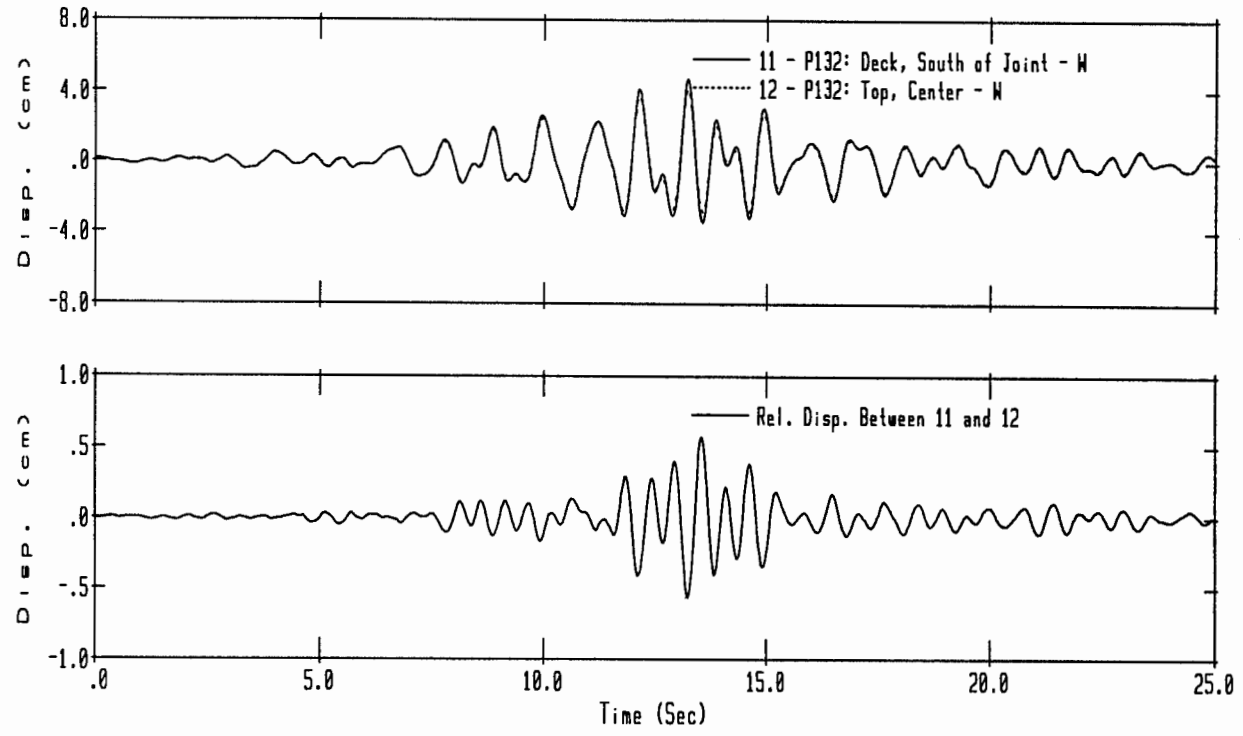

Figure 13 Comparison of Integrated Displacement Time-Histories at Sensors 11 and 12 and the Relative Displacement Time-History Computed from Them

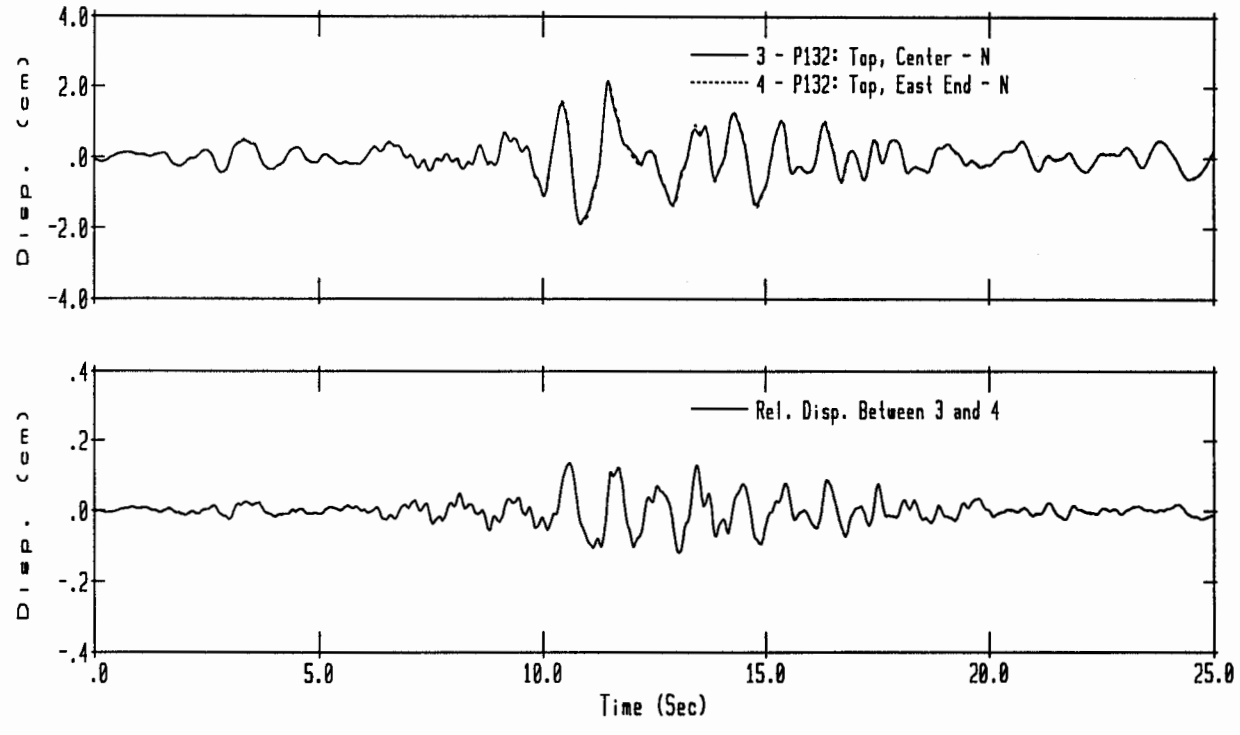

Figure 14 Comparison of Integrated Displacement Time-Histories at Sensors 3 and 4 and the Relative Displacement Time-History Computed from Them

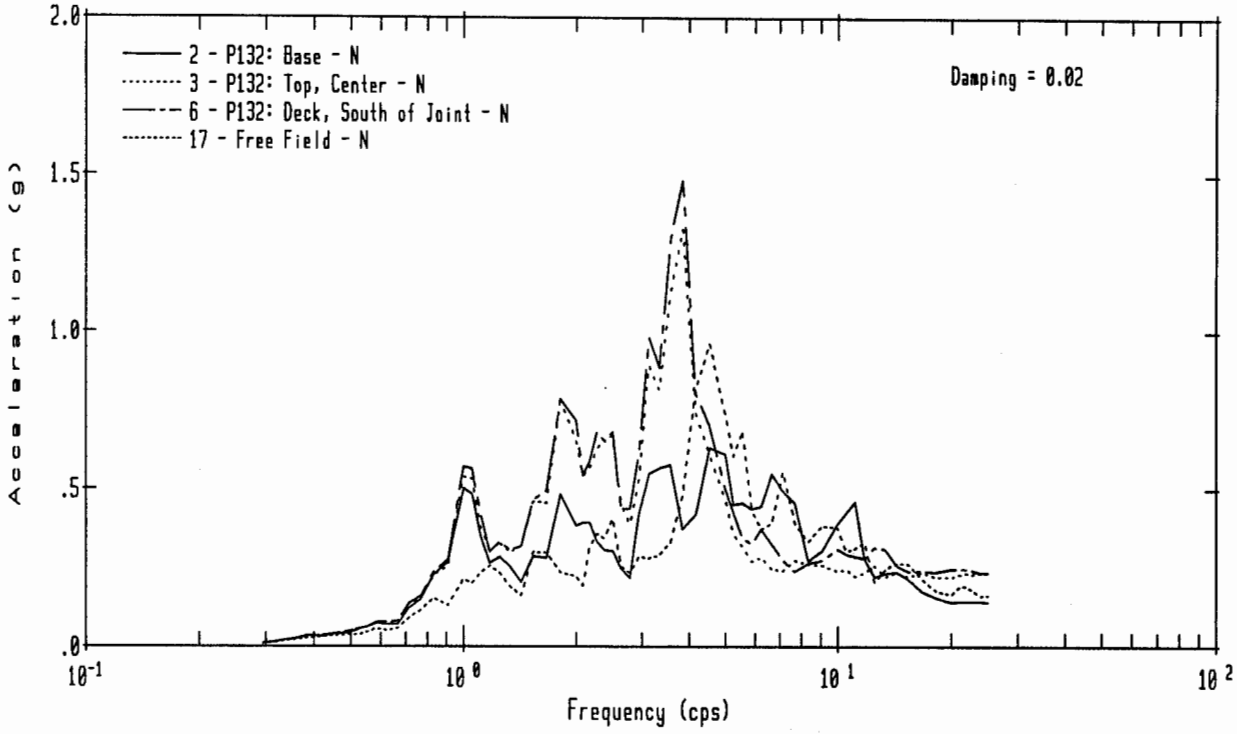

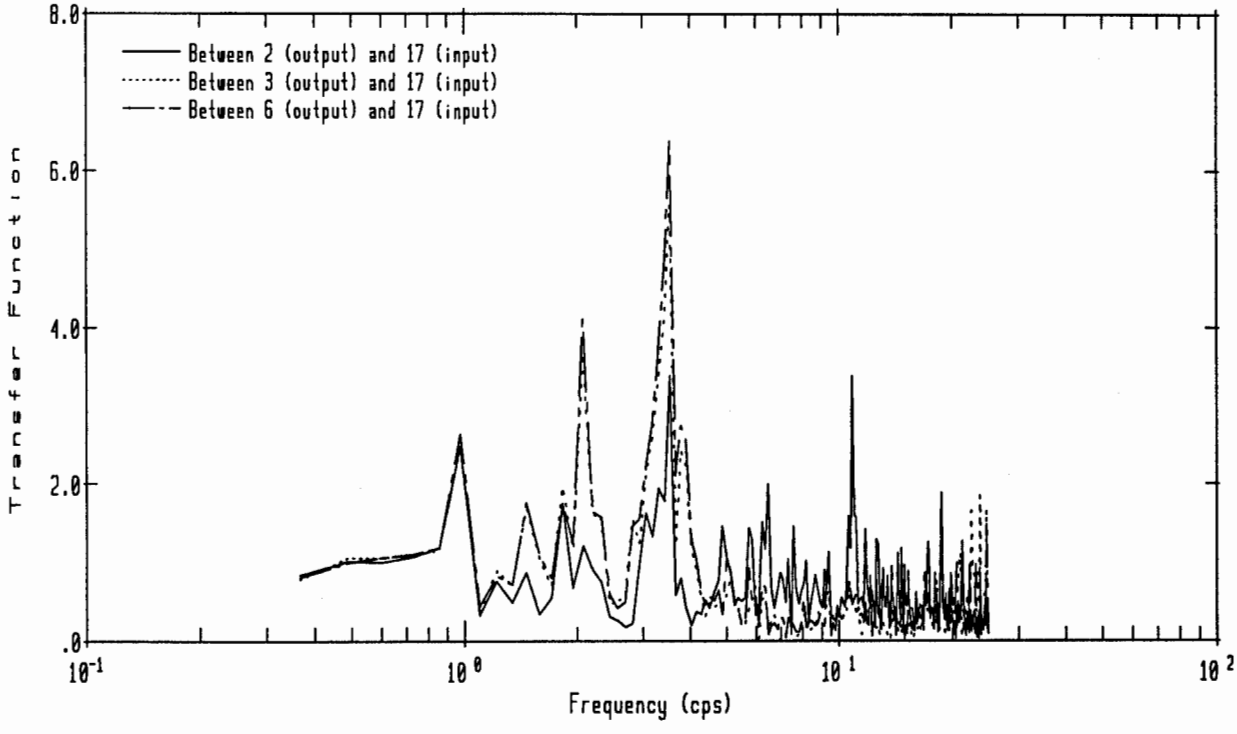

Figure 15 Acceleration Response Spectra of Recorded Longitudinal Response Motions at Pier P132 and Transfer Function Amplitudes Relative to Free-Field

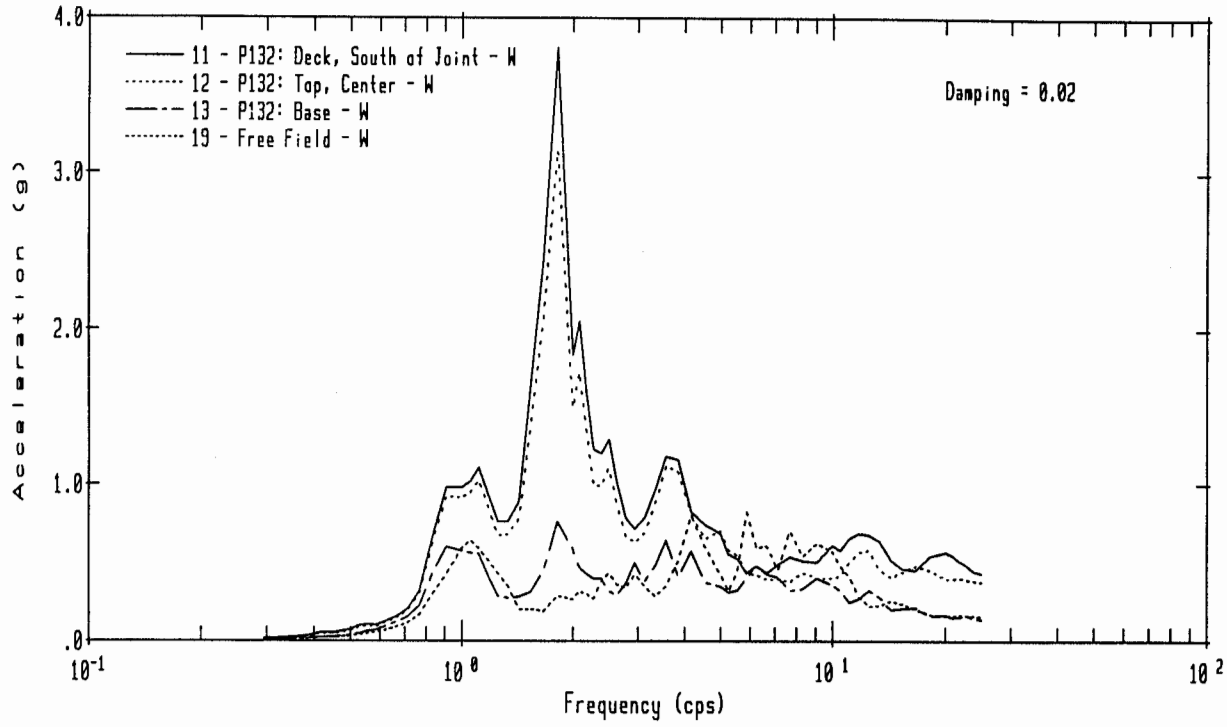

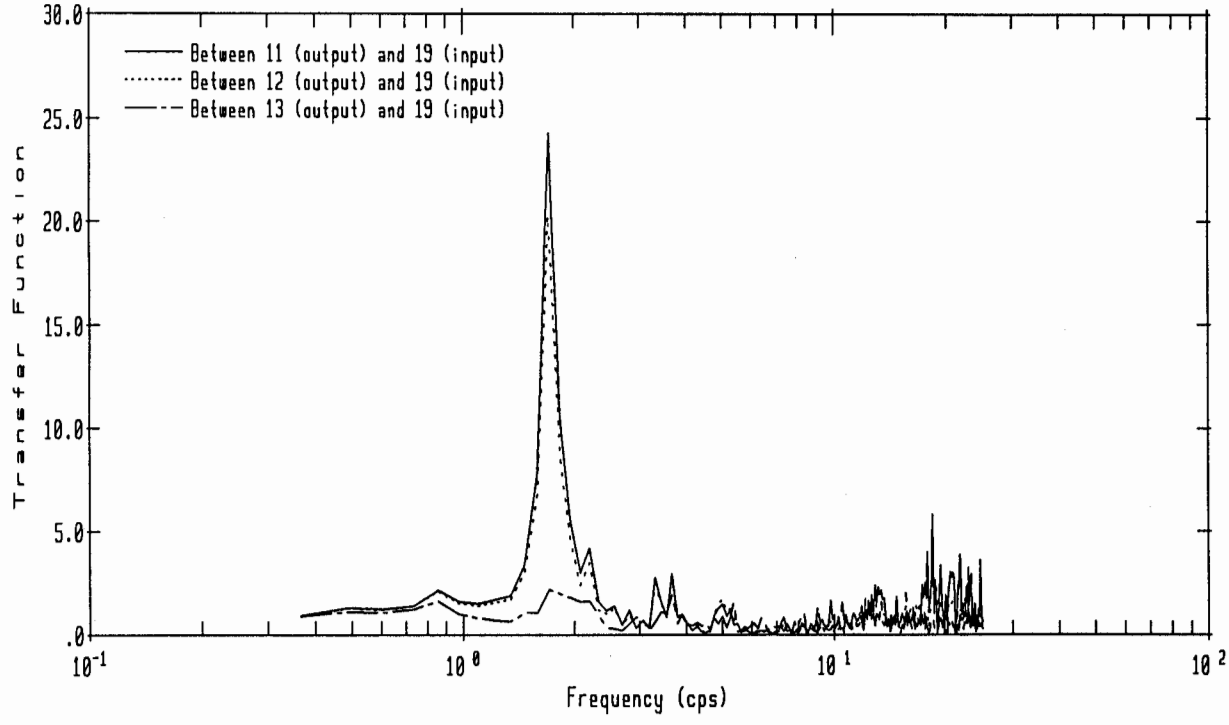

Figure 16 Acceleration Response Spectra of Recorded Transverse Response Motions at Pier P132 and Transfer Function Amplitudes Relative to Free-Field

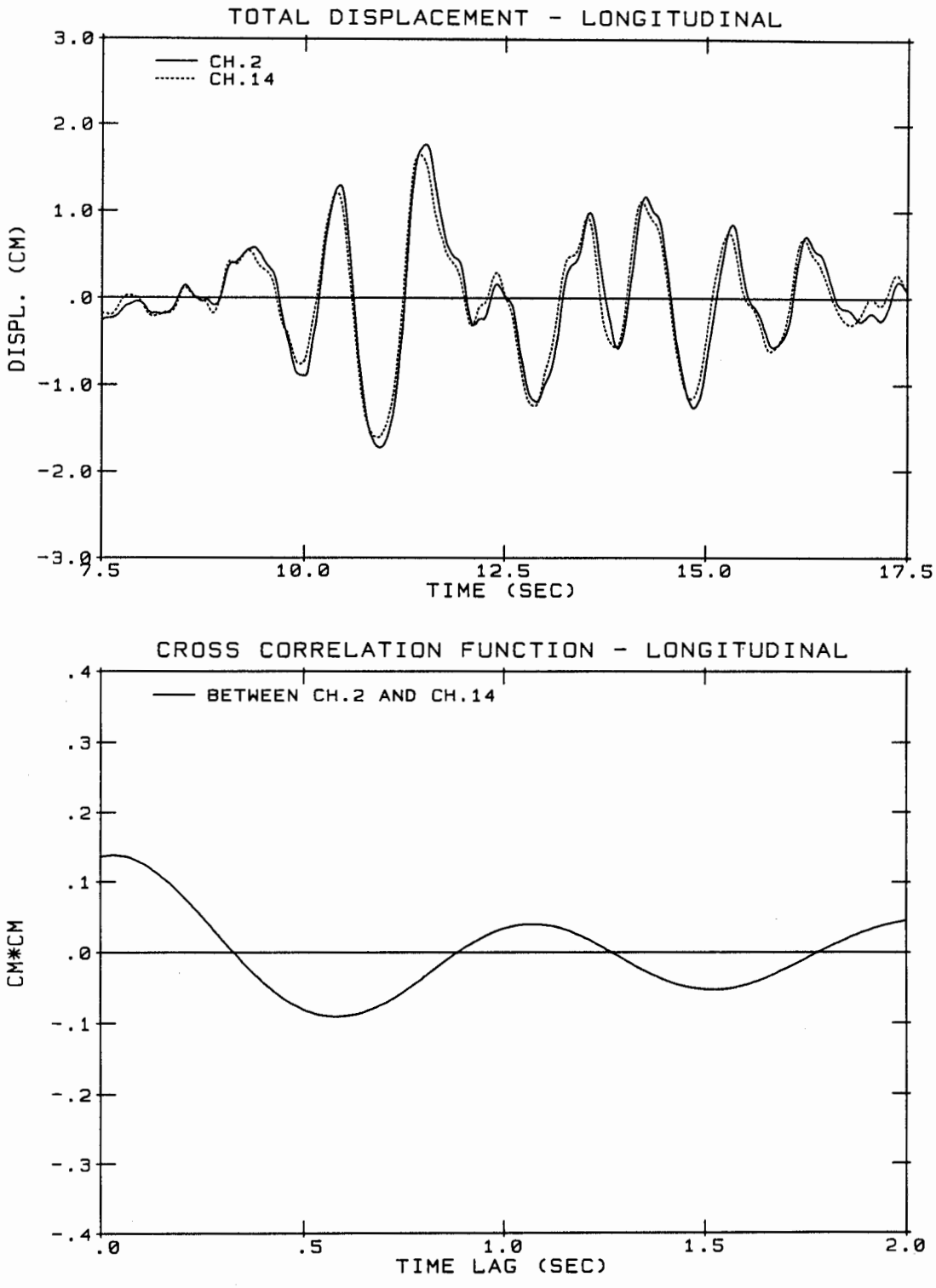

Figure 17 Comparison of Integrated Longitudinal Displacement Time-Histories at Pier Bases of P132 and P135 and Their Cross-Correlation Function

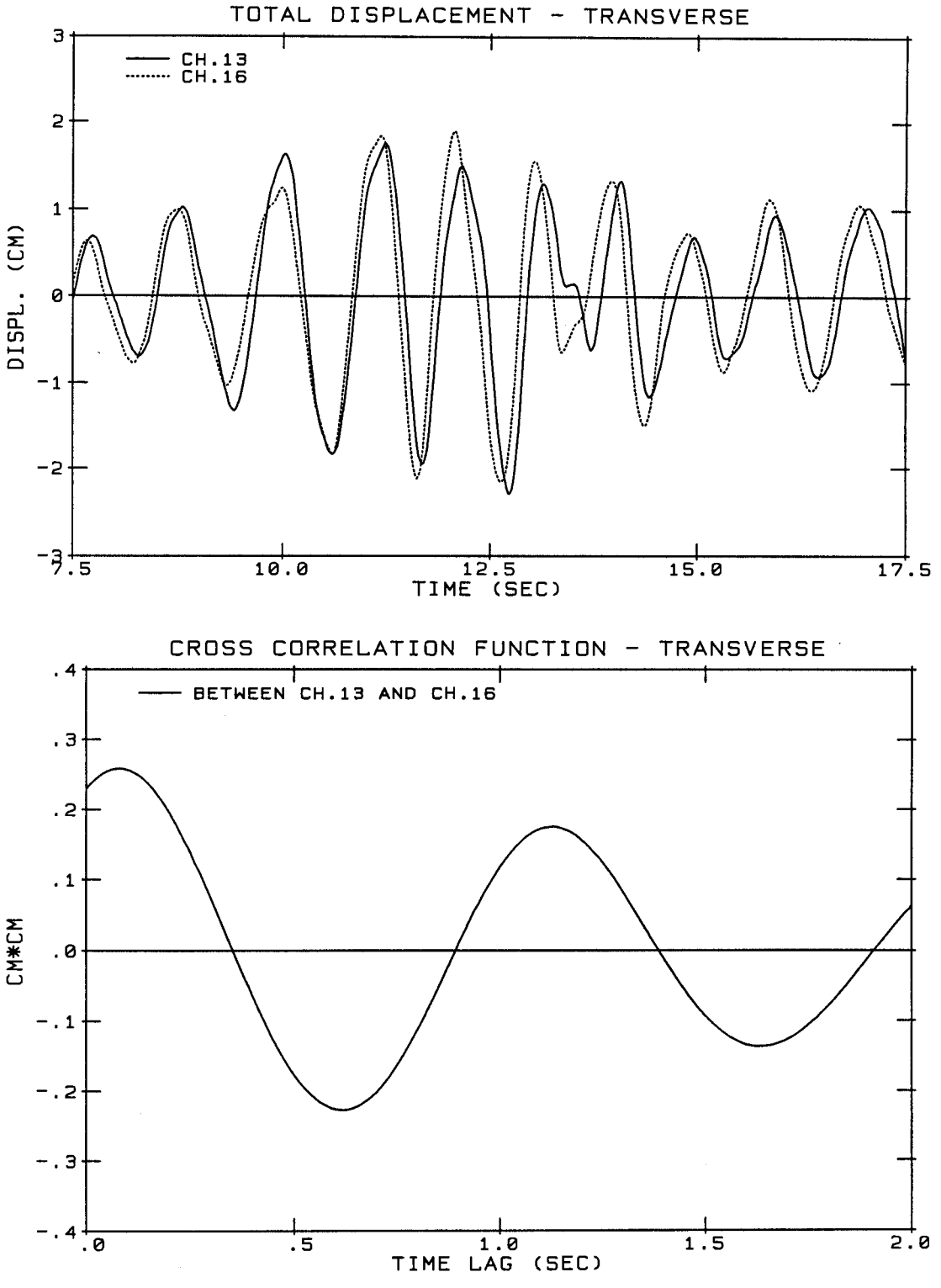

Figure 18 Comparison of Integrated Transverse Displacement Time-Histories at Pier Bases of P132 and P135 and Their Cross-Correlation Function

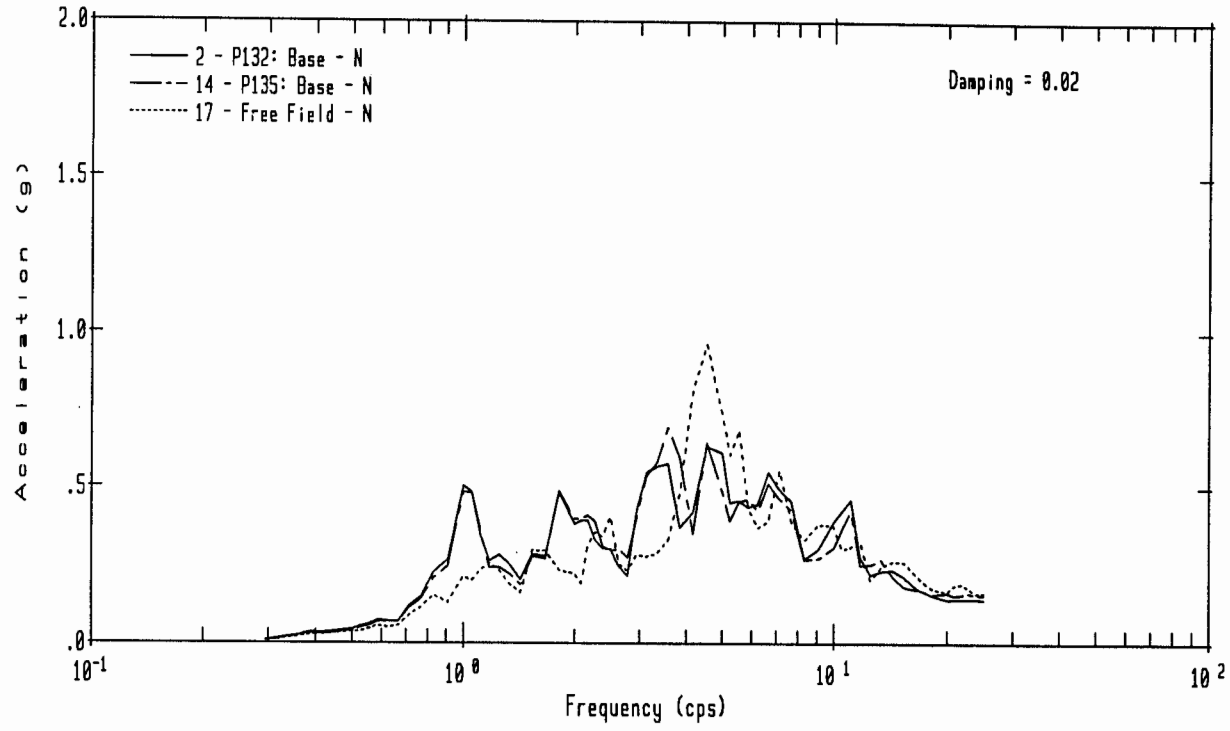

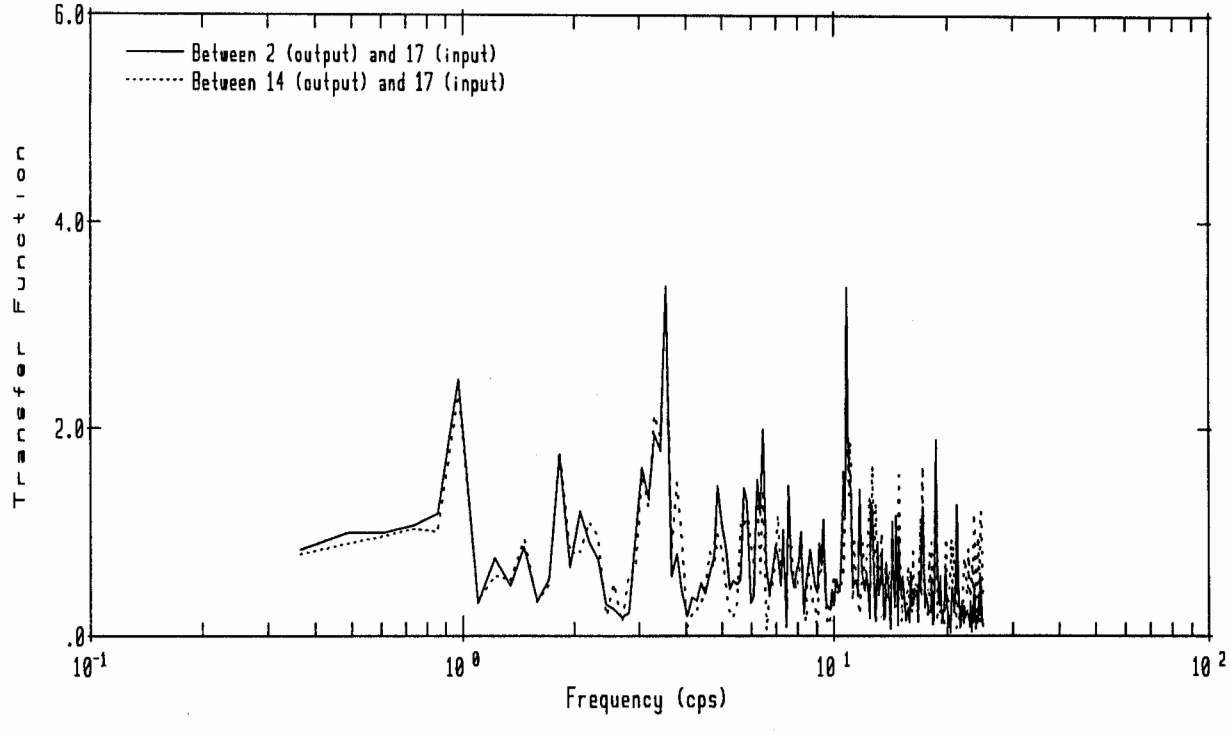

Figure 19 Acceleration Response Spectra of Recorded Longitudinal Base Motions at Piers P132 and P135 and Transfer Function Amplitudes relative to Free-Field Recorded Motion

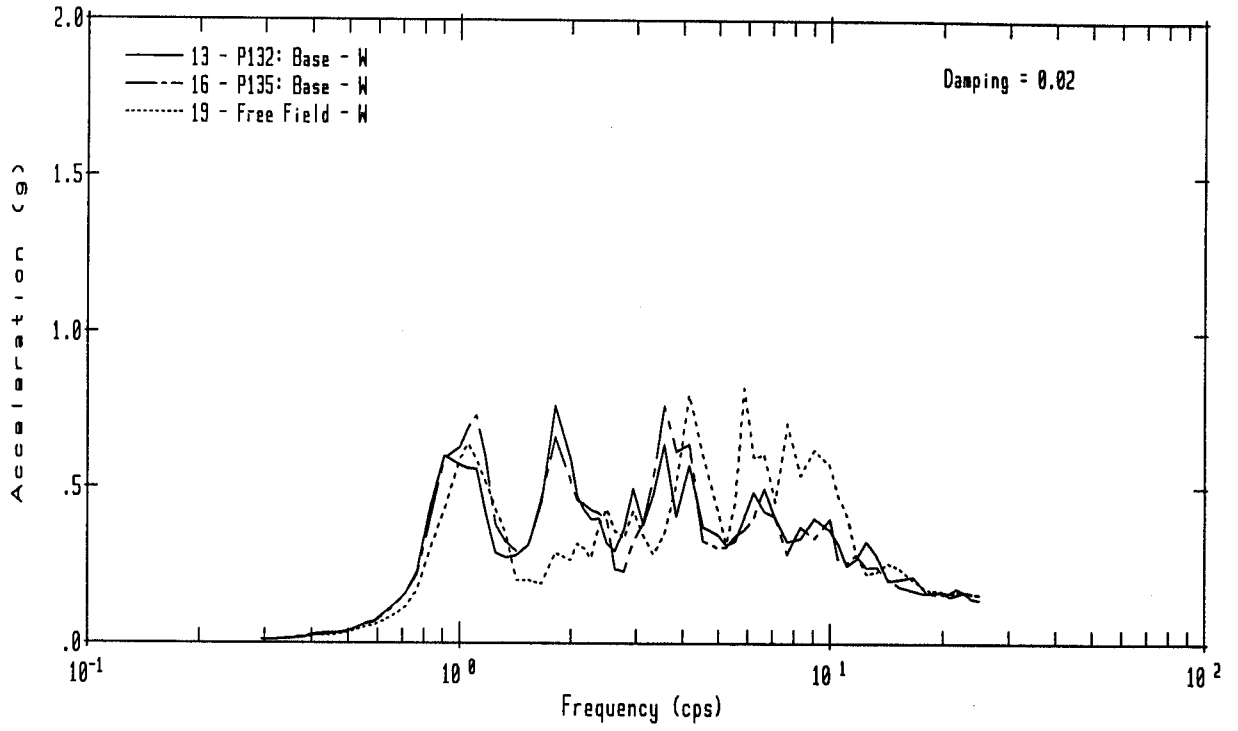

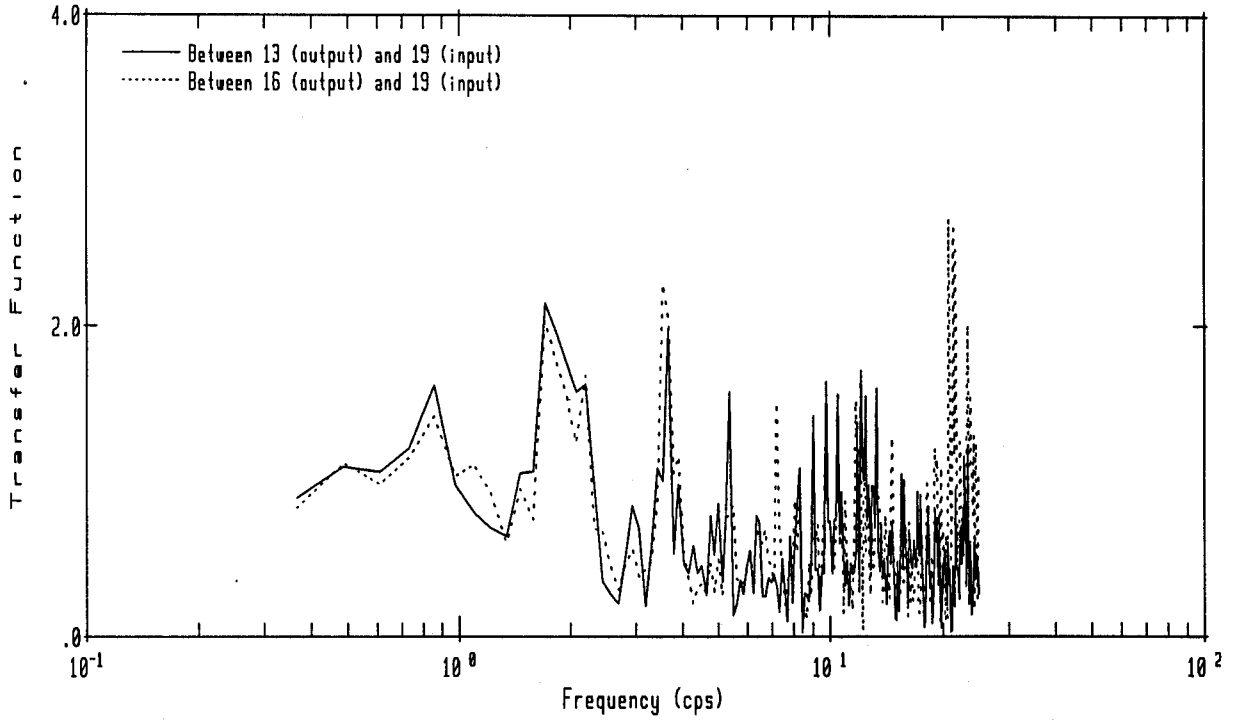

Figure 20 Acceleration Response Spectra of Recorded Transverse Base Motions at Piers P132 & P135 and Transfer Function Amplitudes Relative to Free-Field Recorded Motion

V. DEVELOPMENT OF ANALYTICAL MODELS

Based on the dynamic response behaviors of the structure observed from the results of data analyses described previously, analytical models intended for capturing the observed gross dynamic response behaviors were developed. As described previously, the longitudinal and the transverse structural responses observed from the recorded data show essentially decoupled behaviors, separate longitudinal and transverse models could be used for the structure in capturing its overall behavior. Furthermore, since the structures of all three spans are essentially the same and their observed responses are also quite similar, it is only necessary in developing analytical models to consider the structure and foundation system of a typical span. As pier P132 has been most extensively instrumented, a representative one-span structure tributary to it was used for developing the analytical models. Because the recorded data have indicated significant soil-structure interaction effects, the dynamic impedance characteristics of the pier foundation system were included in developing the analytical models.

Transverse Model

For response prediction in the transverse (EW) direction of the structure, a lumped-mass generalized-beam-stick model was used to represent the one-span structure tributary to pier P132 as shown in Fig. 21. As shown in this figure, the model consists of: 2 lumped masses representing the twin box girders, which

respond essentially as rigid bodies due to their very high fundamental horizontal frequency (10 Hz) relative to the dominant system frequency (1.8 Hz) in this direction; 4 lumped masses representing the pier beam and column; and one lumped mass representing the pier footing (pile cap). For each lumped mass, its tributary rotary inertia is also included. The girder lumped masses are connected to the lumped mass representing the rigid pier beam through two shear springs (K_p) representing the apparent shear stiffnesses of the elastomeric bearing pads. The lumped masses of the column are interconnected by elastic beam elements which have stiffness properties based on the gross uncracked concrete section of the column. The Young's modulus of elasticity used for the pier-column beam elements was obtained using a concrete strength value of 4,000 psi and the ACI formulas. Even though the specified design strength of concrete was 3,000 psi, the higher value of strength selected for the model is intended to take into account the as-built condition, which generally has a higher concrete strength than the specified value, and the effect of concrete hardening with age. The model properties used for the analytical model are summarized in Table 1. The fundamental model frequency of the fixed-base structure obtained from this model is 2.5 Hz with an effective modal mass of approximately 80% of the total structure mass in the model; the second mode frequency obtained is 17.4 Hz with its associated effective modal mass of about 15% of the total mass. Thus, a consideration of the first two modes in the dynamic response analysis would effectively account for about 95% of the total mass of the structure. The modal damping ratios for the fixed-base structure are assumed to be 2.5% for all modes.

The dynamic characteristics of the soil-pile foundation system are represented by a set of frequency-independent foundation impedances (i.e., constant soil springs and dampers). A set of translational soil spring and damper (K_{xx} and C_{xx}) and a set of rocking soil spring and damper ($K_{\theta\theta}$ and $C_{\theta\theta}$) are attached to the pier footing a distance H above the pier footing's center of mass as shown in Fig. 21. This distance H is intended to simulate the effect of foundation embedment which results in increases in the foundation impedance values and creates a coupling impedance ($K_{x\theta}$ and $C_{x\theta}$) between the foundation translation and rocking rotation. The numerical values of the translation and rocking spring stiffnesses (K_{xx} and $K_{\theta\theta}$) were estimated using the result of a pile group test conducted recently by Caltrans (Ref. 3) and the axial stiffnesses of the battered piles. The stiffnesses as obtained were further adjusted considering the soil shear modulus degradation effect due to the free-field soil shear strains induced during the earthquake. The values of the translation and rocking damper coefficients (C_{xx} and $C_{\theta\theta}$) were derived by assuming critical damping ratios of 20% and 15%, respectively, for the rigid body translation and rocking modes of the rigid structure on the flexible foundation. Distance H is left as a parameter to be adjusted in optimizing the correlation between the predicted and measured responses. The final values of foundation impedances selected for the model are shown in Table 2.

Longitudinal Model

For predicting the longitudinal (NS) response of the structure, the

analytical model selected to represent a typical span of structure tributary to pier P132 is essentially the same as that of the transverse model described above; however, recognizing that the structure in the longitudinal direction is highly coupled to the stiffer and much more massive structure of the Hayward BART Station through the high axial stiffnesses of the girders and the rigidly-fastened rails across the girder joints, the longitudinal model for a representative span in coupled longitudinally through two axial links, representing the effective axial stiffnesses of the girders and rails, to a stiffer and more massive model representing the gross dynamic characteristics of the structures of the Hayward BART Station immediately to the south as shown in Fig. 22. Since the recorded data indicate that the longitudinal structure responses throughout the 3-span structure have a dominant response frequency at about 3.5 Hz and a minor response frequency at about 2.1 Hz, it is postulated that the frequency at 3.5 Hz is dominated by the stiffer Hayward BART Station structure. Thus, the model properties of the stiffer model representing the Hayward BART Station were adjusted to reflect a fundamental frequency in the longitudinal direction of about 3.5 Hz.

Table 1

Model Properties of Transverse Analytical Model

Node Number	Elevation (ft)	Mass (k-sec^2/ft)	Mass Moment of Inertia (k-ft-sec^2)	Element Properties		
				Connectivity	A (ft^2)	I (ft^4)
1	116.73	7.6	73.1	1-3	K_p	-
2	116.73	7.6	73.1	2-4	K_p	-
3	115.69	0	0	3-5	Rigid	Rigid
4	115.69	0	0	4-5	Rigid	Rigid
5	113.51	2.18	79.31	5-6	Rigid	Rigid
6	110.69	.59	0	6-7	32.02	58.34
7	100.34	1.18	0	7-8	32.02	58.34
8	90.00	.59	0	8-9	Rigid	Rigid
9	87.07	6.11	139.2			

Notes: (1) Young's Modulus of Concrete = 520,000 ksf
(2) Nodes 1, 2, 3, and 4 are constrained to Node 5 to have the same rotation.
(3) Girder Bearing Shear Spring K_p = 12,100 k/ft

Table 2

Properties of Transverse Analytical Model Foundation Impedance

Soil Springs:	
Translation	K_{xx} = 18,000 k/ft
Rocking	$K_{\theta\theta}$ = 1.15 x 10^7 k-ft/rad.
Soil Dampers:	
Translations	C_{xx} = 270 k-sec/ft
Rocking	$C_{\theta\theta}$ = 1.27 x 10^5 k-ft-sec/rad
Impedance Attachment Position:	
H = 2.25 feet above C.G. of footing (see Fig. 21)	

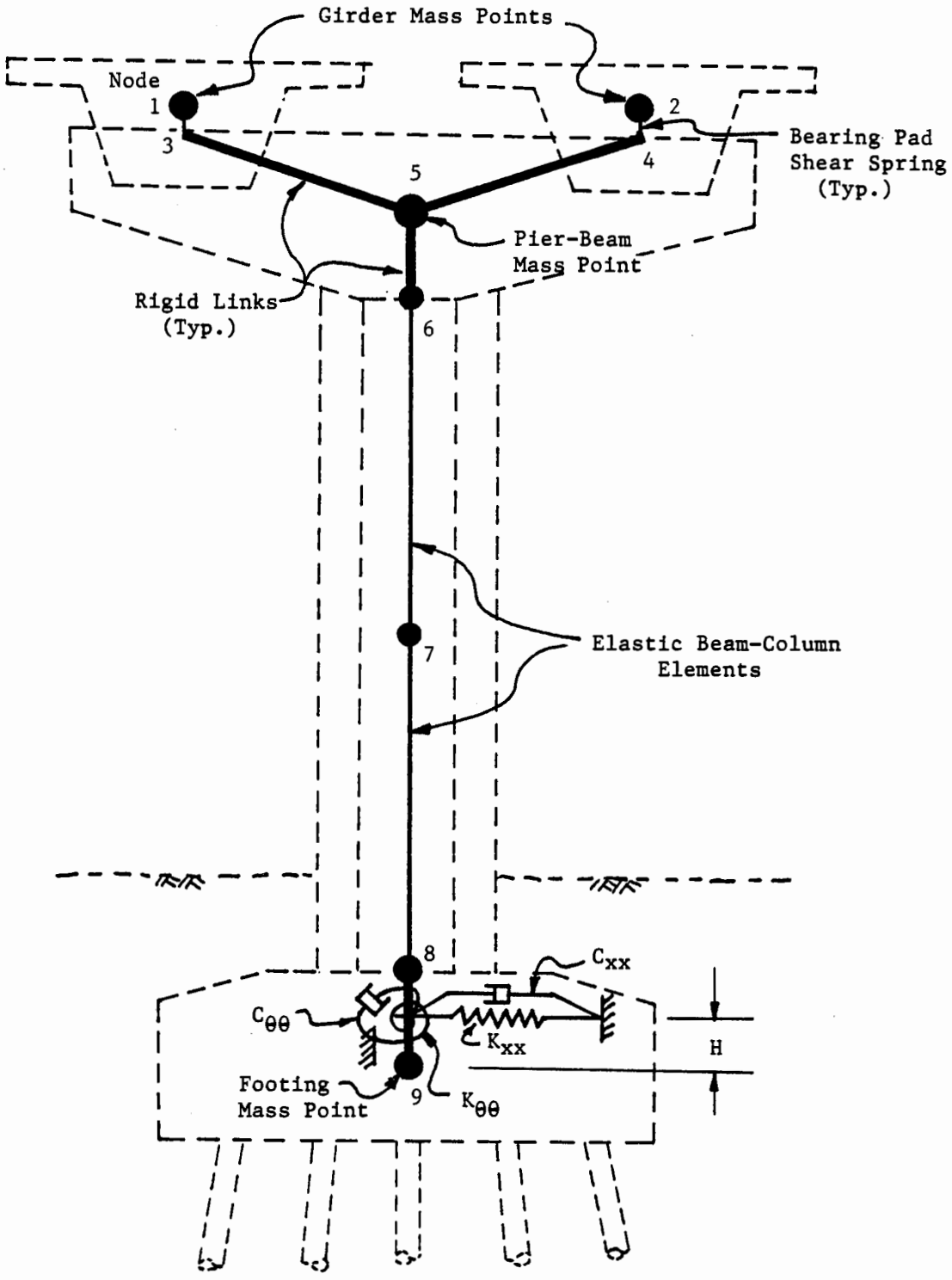

Figure 21 Analytical Model for the Transverse Response Analysis

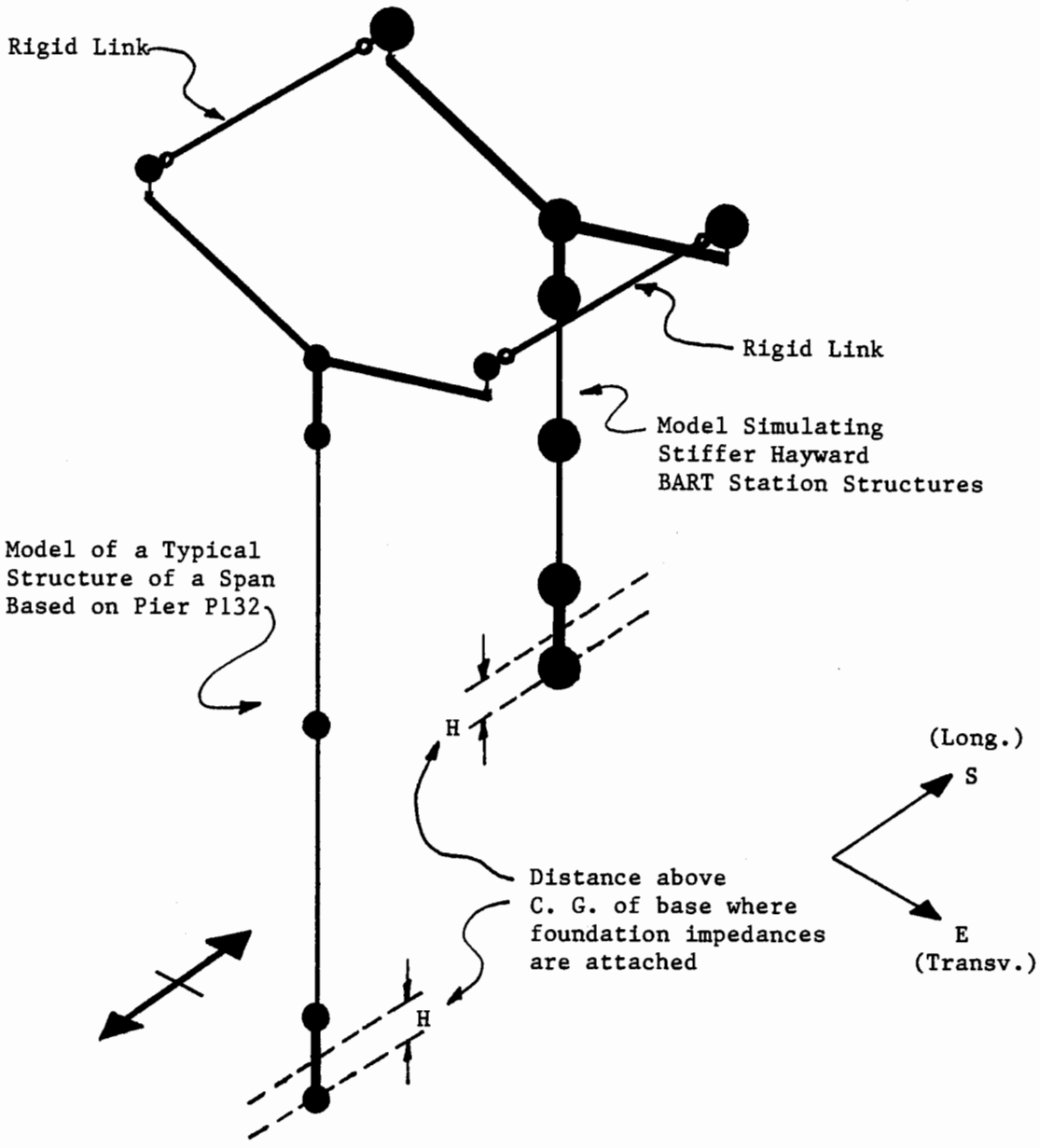

Figure 22 Analytical Model for the Longitudinal Response Analysis

VI. CORRELATION OF ANALYTICAL AND MEASURED RESPONSES

Based on the longitudinal and transverse analytical models developed as described previously, dynamic responses of the models subjected to the inputs of the free-field acceleration time-histories in the NS and EW directions as recorded by the free-field Sensors 17 and 19, respectively, were computed. Since model parameters such as soil and elastomeric material properties are uncertain and since the recorded data are not sufficient to deduce the needed information, numerous parametric variations were considered in the analysis. Included in these parameter variations were the stiffnesses of the elastomeric bearing pads, the foundation soil modulus and damping values, and the distance H used in characterizing the foundation embedment effect. The final values of these parameters were selected as those which resulted in the best correlations between the analytically predicted responses and the corresponding measured responses.

The responses obtained from analyses using the best-estimate parameter values are compared with the corresponding measured responses in the form of 2%-damped acceleration response spectra calculated from the acceleration response time-histories and the transfer function amplitudes of the calculated response motions relative to the free-field input motions. These comparisons and discussions of the results are summarized below.

Longitudinal Responses

The 2%-damped acceleration response spectra for the analytically computed longitudinal response motions at sensor locations 6 (girder), 3 (pier beam), and 2 (pier base) are compared with the corresponding spectra for the measured response motions in Fig. 23. The analytically computed transfer functions between the Fourier amplitudes of free-field input and the Fourier amplitudes of structural responses shown in Fig. 24 can be compared to the corresponding results obtained from the measured responses shown previously in Fig. 15. These comparisons indicate that the analytical results capture the dominant response behavior of the structure at the frequency of 3.5 Hz reasonably well; however, they are deficient in predicting the minor responses at the frequencies of 1 Hz and 2.1 Hz. The transfer functions were generated using the five-point segment averaging procedure.

The rather narrow-band character of the longitudinal responses centered around 3.5 Hz is attributable to a similar system frequency of the stiff Hayward BART Station structure. A future confirmation of this response characteristic is desirable; however, to make this possible would require shifting some of the recording sensors toward the structure of the Hayward BART Station.

Transverse Responses

The 2%-damped acceleration response spectra for the analytically-predicted

transverse response motions at sensor locations 11 (girder), 12 (pier beam), and 13 (pier base) are compared with the corresponding results obtained from the measured response motions in Fig. 25. Figure 26 shows the transfer function amplitudes obtained from the analytical model. These amplitudes can be compared with the corresponding results as shown previously in Fig. 16. As indicated by these comparisons, the transverse analytical model captured the fundamental model response at the frequency of 1.8 Hz very well; however, it is somewhat deficient in predicting the second mode response at the frequency of 3.6 Hz, which is basically due to the foundation rocking. Because of the lack of recorded data that could be used in separating the rocking components and translation component of the pier base motions, further refinements of the foundation model, which significantly controls the transverse structural response behavior, could not be achieved rationally. Thus, a future installation of sensors capable of independent recordings of data of the rocking motions of the pier bases are most desirable.

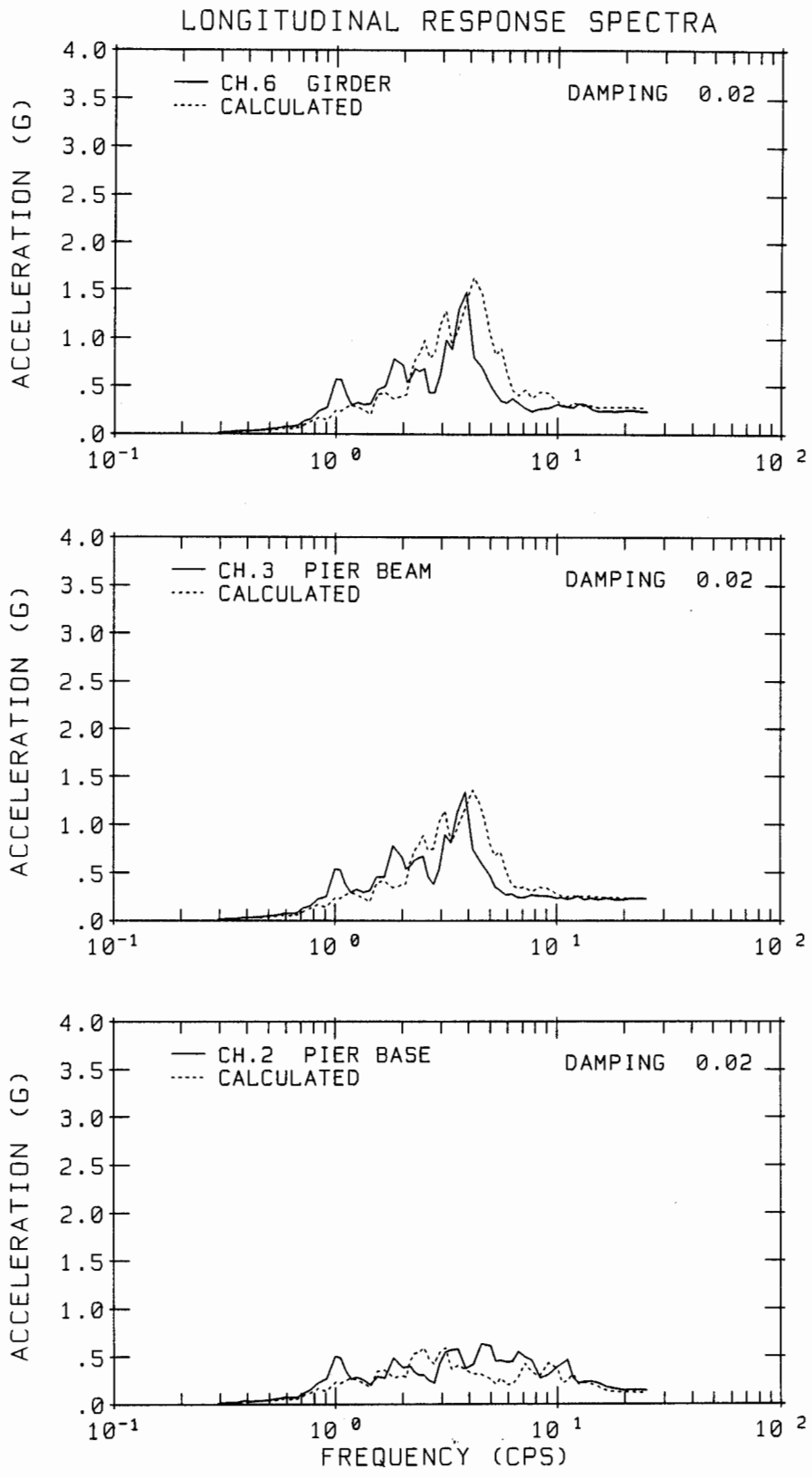

Figure 23 Comparisons of Analytically-Predicted and Measured Responses

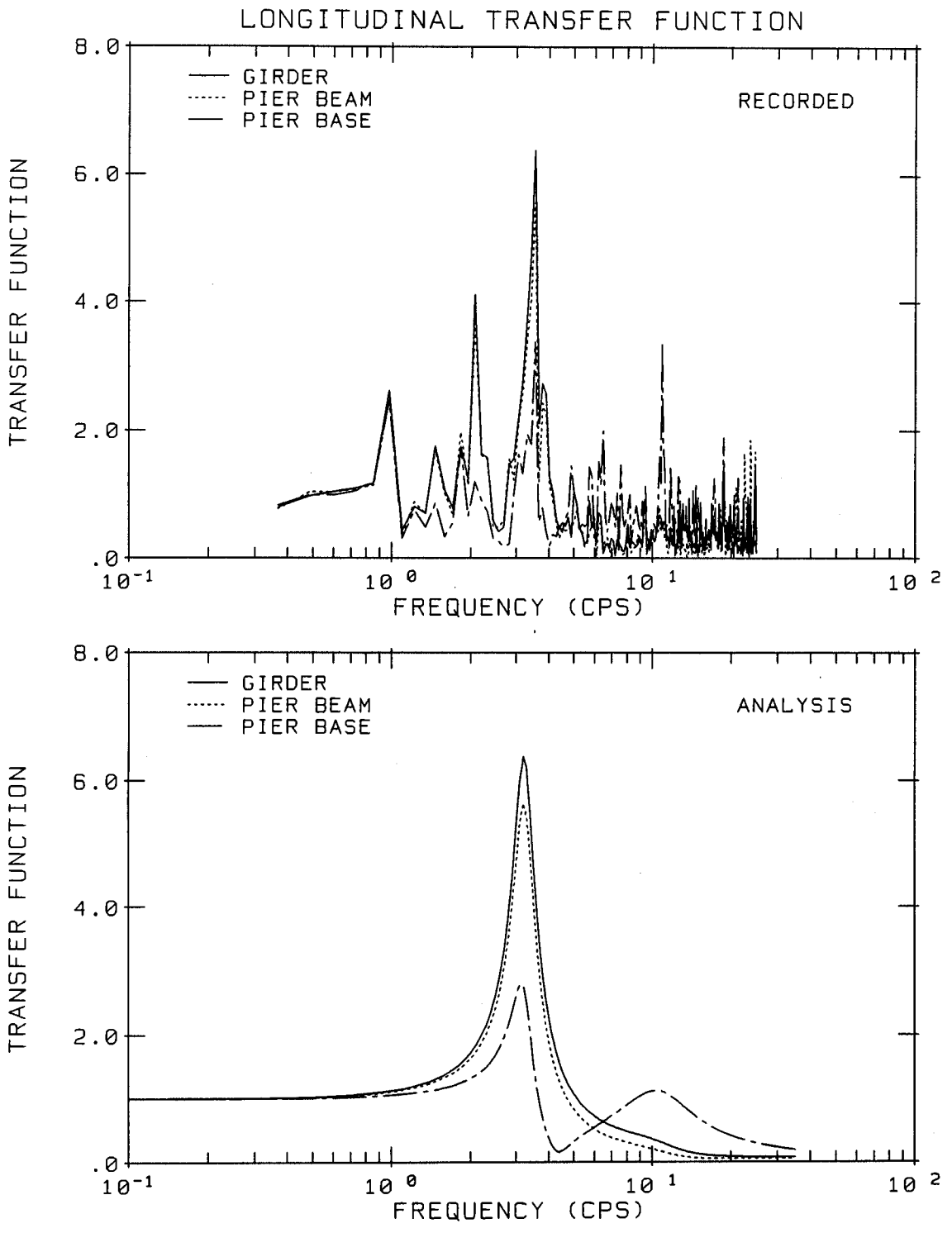

Figure 24 Comparisons of Analytically-Computed and Recorded-Data-Deduced Transfer Function Amplitudes for the Longitudinal Response at P132

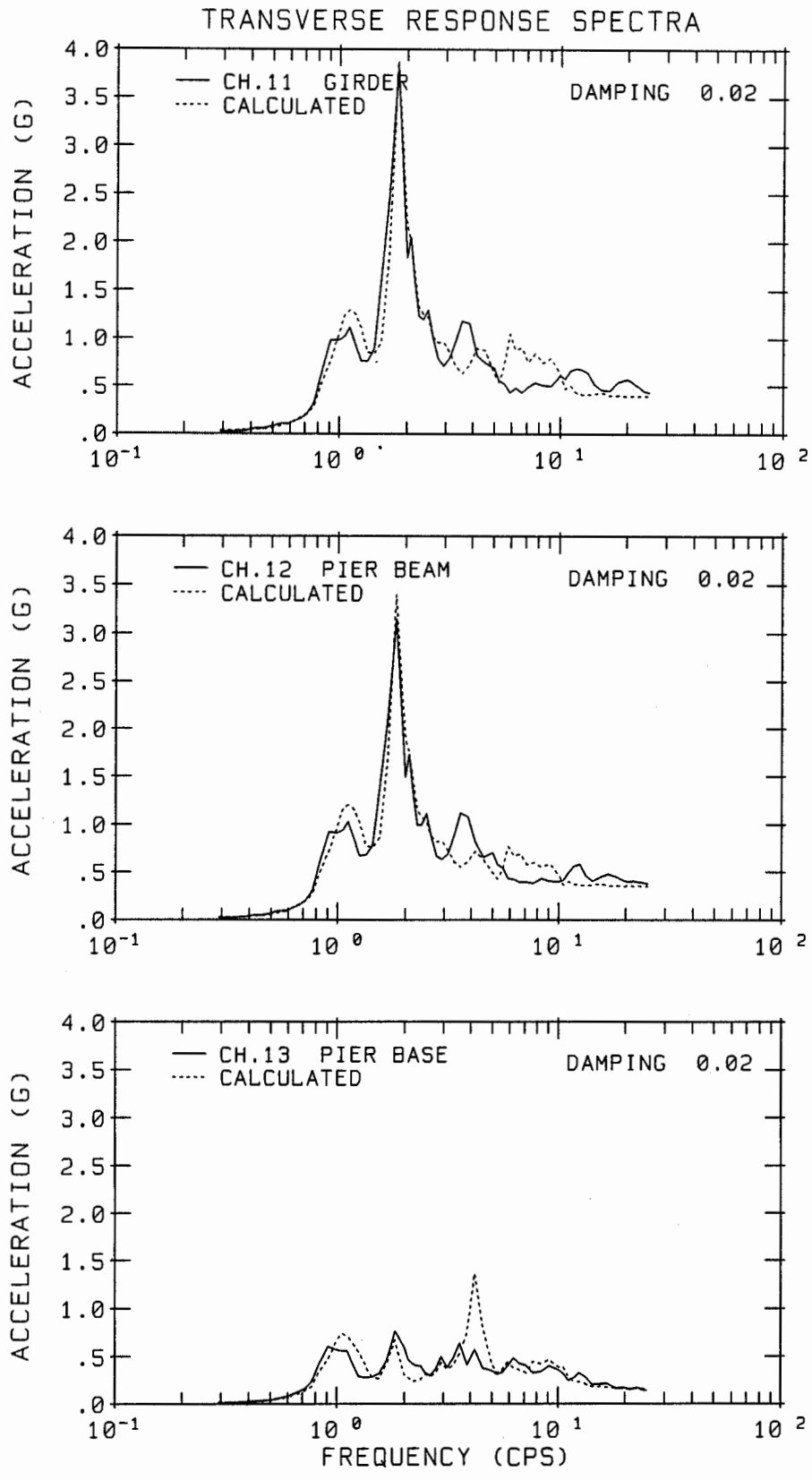

Figure 25 Comparisons of Analytically-Predicted and Measured Responses

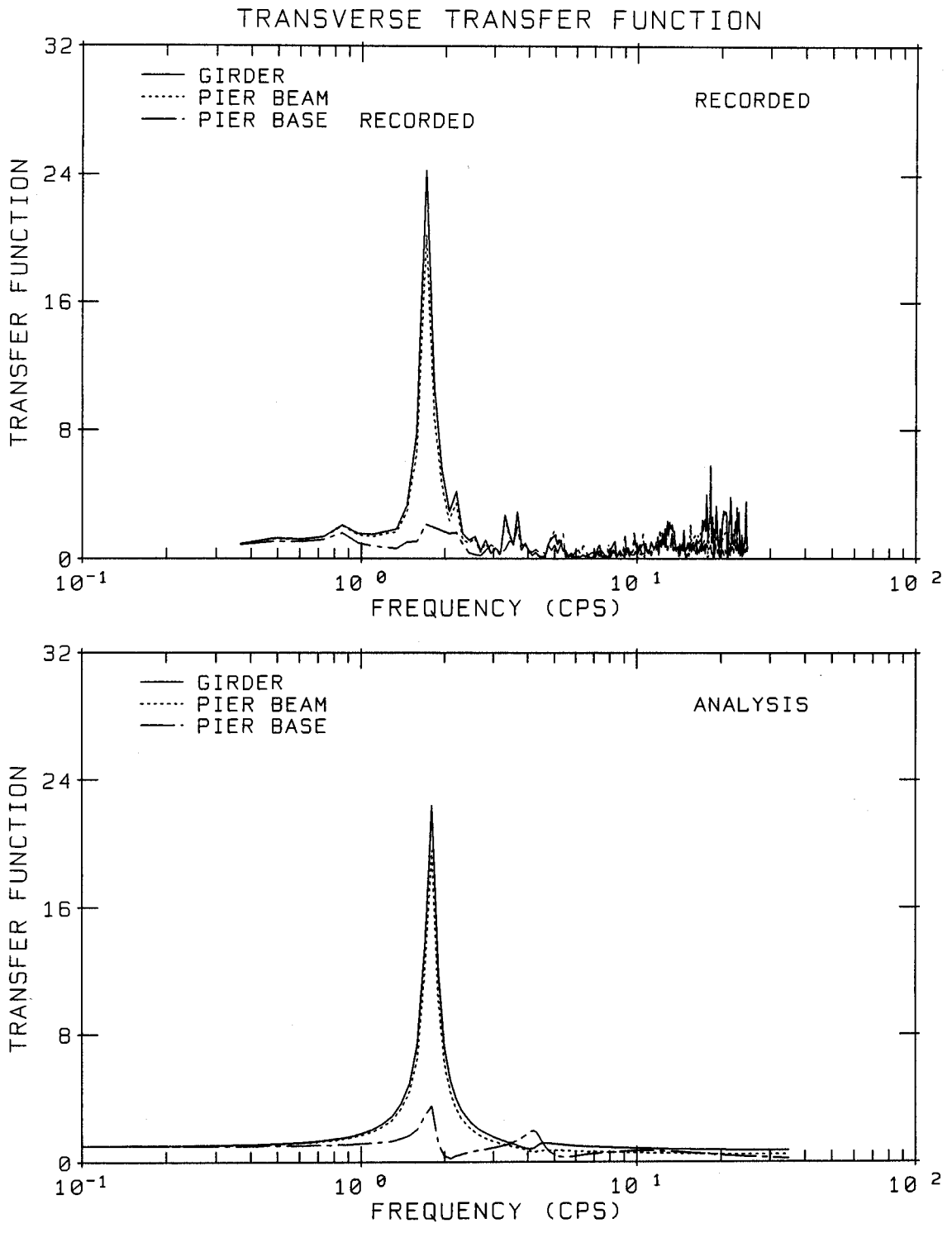

Figure 26 Comparisons of Analytically-Computed and Recorded-Data-Deduced Transfer Function Amplitudes for the Transverse Response of P132

VII. ASSESSMENT OF STRUCTURAL PERFORMANCE AND DESIGN IMPLICATIONS

The earthquake response data recorded at the three-span section of the Hayward BART elevated structure offer a unique opportunity to assess the seismic performance of this structure during the Loma Prieta earthquake. From the results of this assessment, implications on design procedures of current engineering practice can be drawn. Furthermore, using the analytical models developed from the correlation study as described previously, a gross assessment can be made of the expected performance of this structure at the seismic input level of the maximum credible earthquake (MCE) condition currently specified for design in the BART Extension Program. In conducting these assessments, emphasis is placed on the more critical transverse responses of the structure since they control its design and they are the more representative response of a typical BART elevated structure; whereas the longitudinal response of the structure is less representative due to the influence of its close proximity to the Hayward BART Station.

The maximum seismically-induced moment in the transverse direction at the column base of pier P132 during the Loma Prieta event can be obtained approximately by taking the maximum value of the column-base moment time-history obtained from the sum of the products of the tributary masses with their recorded transverse acceleration time-histories and the associated distances from the mass points to the column base. Based on this calculation, the maximum transverse moment at the pier-column base is about 5,800 k-ft. This maximum moment

predicted by the transverse analytical model for the structure-foundation system of pier P132 developed for the correlation study described previously is about 6,000 k-ft, which agrees quite well with the value of 5,800 k-ft estimated directly from the recorded data. On the other hand, this maximum moment is predicted by the transverse analytical model having a fixed-base condition, as normally assumed in design, is only about 4,000 to 4,400 k-ft, i.e., approximately a factor of 1.3 to 1.5 smaller than the value predicted including soil-structure interaction effects.

The ultimate base-moment capacity in the transverse direction of the column of pier P132 which has 44-#18 Grade 40 rebars at its base, under the dead load of 630 kips, was determined to be about 12,500 k-ft. Thus, the maximum transverse moment demand at the column base during the Loma Prieta earthquake was approximately 45 percent of the column capacity, which explains why this section of structure was undamaged during the earthquake.

In order to assess the seismic performance of the structure under the MCE seismic input level (PGA = 0.7g) currently used for design in the BART Extension Program, the transverse analytical model for the structure-foundation system of pier P132 was subjected to the seismic input of a design-response-spectrum-compatible artificial acceleration time-history normalized to the PGA value of 0.7g, as shown in Fig. 27; and, its seismic response was calculated. In this analysis, the fixed-base structure modal damping ratios were all assigned the value 0.05 instead of the value 0.025 used in the correlation study for the Loma

Prieta event. This increase of damping was introduced in recognition of the higher damping ratios present at the response levels produced by the 0.7g seismic event. Since a precise estimate of the foundation damping values at the 0.7g level of input is not possible due to the lack of site-specific information on dynamic soil properties, a range of foundation damping ratios were considered in the analysis, namely, values in the range of 20-30% for the rigid body translation mode and 15-20% for the rigid body rocking mode. The results of this linear analysis indicate that the maximum transverse moment induced at the column base is in the range 50,400 to 63,400 k-ft which has values exceeding the base-moment capacity by a factor of about 4. A corresponding linear analysis assuming a fixed-base condition gives the corresponding base-moment demand at 28,000 k-ft, which is lower than the values obtained including soil-structure effects by a factor of about 1.8 to 2.3.

The above estimate of base-moment demand for the linear structure/foundation model using the 0.7g level of seismic input is certainly an upper-bound estimate since, as the demand exceeds the capacity, column stiffness degradations result; furthermore, at this high level of input, the foundation stiffnesses also degrade due to the nonlinear soil-pile behavior; both of these effects would result in a shifting of the system's frequencies to a lower frequency range which had reduced spectral amplifications (see Fig. 27) and an associated increase in the system's damping due to the system's increased energy dissipations, leading to a further reduction of response using equivalent linear modelling.

From the results of analyses presented above and the observations of the seismic response behavior of the structure as described previously, valuable insights into the seismic performance of this section of the BART elevated structure have been obtained and their implications on design have been assessed as follows:

(1) The apparent structural damping value of the BART structure, as indicated from the recorded data and as found to give reasonable correlations, is about 2.5% for the fixed-base structure and about 4% for the structure-foundation composite system, both of which are lower than the value of 5% normally used in design. This lower apparent damping value leads to a structural response amplification factor at the deck level of about 4 which is higher than the peak elastic spectral amplification factor of 3 normally used for design. However, considering that the peak horizontal acceleration of the free-field motions during the earthquake was only 0.16g, the damping value of 5% and the peak elastic spectra amplification factor of 3 at the design seismic input level of 0.35g to 0.7g for the BART structure can be judged to be reasonable and conservative for design purposes.

(2) As indicated by the recorded data, as well as by the parametric correlation studies, the soil-structure interaction effect on seismic response of the structure is significant. This effect tends to lower the structural system frequencies appreciably. For example, the analytical model developed for the transverse response prediction shows the fundamental fixed-base

structural frequency to be 2.5 Hz which is considerably above the system frequency of 1.8 Hz obtained when soil-structure interaction is considered. In the design of the BART structure, a fixed-base structural model is normally used which tends to over-estimate the frequencies and under-estimate the response. For the Loma Prieta earthquake, this modelling approach under-estimates the response approximately 25 to 35 percent.

(3) During the Loma Prieta earthquake, the maximum seismically-induced column base moment in the more critical transverse direction was approximately 45 percent of the column's ultimate moment capacity. However, using the input of a design-response-spectrum-compatible accelerogram normalized to the Maximum Credible Earthquake condition having a PGA level of 0.7g, as currently specified in the BART Extension program, the maximum induced column base moment predicted by the equivalent linear model calibrated in this study and adjusted by judgment to account for the effect of system nonlinearities was found to exceed the moment capacity by a factor of about 4. Because the predominant frequencies in the base-moment time-history are centered around 1.8 Hz, the pier ductility demand in flexure will be approximately equal to the base-moment demand given by analysis of the linear structure foundation model; thus, a pier ductility demand of about 4 is indicated for the maximum credible earthquake condition. While this ductility demand produces flexure cracking of the pier, it does not exceed the ductility capacity which is believed to be in the range 6 to 8.

(4) The recorded data indicate that the BART elevated structures are highly coupled in the longitudinal direction due to the presence of the continuous rails which are rigidly fastened to the girders, even though the structure of each span is designed to be simply-supported and free to move at one end. This implies that the single-pier model used for design in this direction may not be appropriate, especially for those elevated sections which have large variations in the pier column heights. When the system is strongly coupled longitudinally, the shorter columns with their higher lateral stiffnesses tend to experience higher seismically-induced internal forces; whereas the single-pier model without this coupling may not predict such a result. Thus, in such situations, a model consisting of structures of several spans and piers may be necessary. Furthermore, due to the apparent strong coupling of the rails, the axial forces induced in the rails across the girder joints should be assessed in such situations.

(5) As discussed previously, the apparent shear stiffnesses of the elastomeric bearing pads for the BART girders have been found to be higher than the code values, indicating potential degradation of the material due to aging or other environmental effects. It would be very useful, if and when these pads are replaced, to perform tests of the existing pads to determine their properties. Furthermore, since their properties in the current condition are uncertain, design or assessment of the structure should consider a wide variation of these properties.

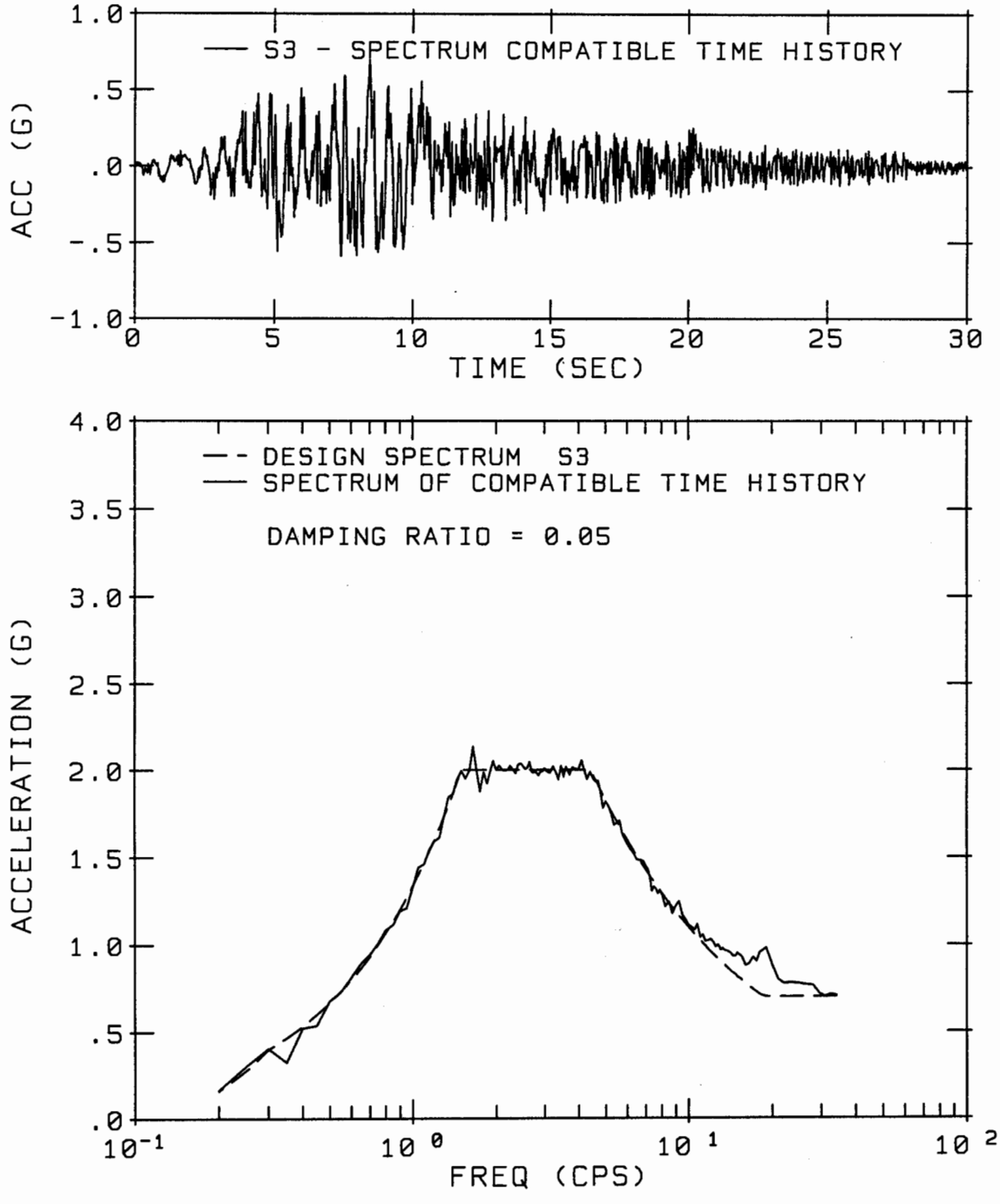

Figure 27 BART Extension Program Design Response Spectrum S3 and Its Spectrum-Compatible Acceleration Time-History Used in Performance Assessment

VIII. CONCLUSIONS AND RECOMMENDATIONS

Based on the analysis and structural performance assessment results obtained in this study, the following conclusions and recommendations can be made:

(1) The data recorded during the Loma Prieta earthquake by the CSMIP instruments on the Hayward-BART elevated structure provide valuable information for understanding the seismic response of this structure.

(2) Due to the high axial stiffness of the continuous rails, the seismic response behavior of this structure in the longitudinal direction was found to be quite different from that in the transverse direction. The former behavior is controlled by the response of the entire coupled system; whereas the latter is more or less controlled locally from span to span. The responses in both directions are significantly influenced by soil-structure interaction effects. In the more critical transverse direction, these effects actually result in higher responses than those obtained using the fixed-base design analysis procedure by a factor of 1.3 to 1.5.

(3) During the Loma Prieta earthquake, the maximum seismically-induced column base moment was approximately 45 percent of the column's ultimate moment capacity. However, using response-spectrum-compatible accelerograms normalized to the Maximum Credible Earthquake PGA level of 0.7g, as currently specified in the BART Extension Program, the maximum induced

seismic base moment predicted by the linear models calibrated in this study was found to exceed the design moment capacity by a factor of about 4. This corresponds to a pier ductility demand of about 4 which is less than its ductility capacity estimated to be in the range 6 to 8.

(4) Since the soil-structure interaction effect is shown to be important, design procedures for estimating the pile foundation impedances and capacities, such as those published in Ref. 4, should be evaluated using actual earthquake response data. However, to make this possible, more instruments should be placed on the foundation base such that they can produce sufficient data for evaluating separate modes of foundation response. The current CSMIP instrumentations are not sufficient for such an evaluation.

(5) The studies conducted point out an urgent need of instrumentation that allows independent recordings of the rocking rotation responses at the bases of pier columns. A need also exists to obtain longitudinal response data at locations closer to the Hayward BART Station. Thus, the current instrumentation layout on this section of structure can be improved by shifting some of the redundant sensors for recording the longitudinal motions of girders to pier bases for measuring base rocking motions and to locations closer to the Hayward BART Station for measuring the longitudinal motions.

(6) The free-field recording instrument (Sensors 17, 18, and 19) is located about 640 feet south and 450 feet west of P135. Consideration should be given to moving this instrument much closer to the Hayward BART structure, but not so close as to experience significant soil-structure interaction effects.

(7) The findings of this study suggest the need for an assessment of current design procedures, including modelling for seismic response predictions and criteria for setting limits on ductility demands.

IX. REFERENCES

(1) Penzien, J. and Tseng, W. S., "Analytical Investigations of the Seismic Response of Tall Flexible Highway Bridges," Report No. UC-EERC 73-12, Earthquake Engineering Research Center, University of California, Berkeley, June 1973.

(2) Shakal, A., Huang, M., et al., "CSMIP Strong-Motion Records from the Santa Cruz Mountains (Loma Prieta), California Earthquake of 17 October 1989," Report No. OSMS 89-06, California Strong Motion Instrumentation Program, California Department of Conservation, Division of Mines and Geology, November 17, 1989.

(3) Abcarius, J. L., "Lateral Load Tests on Driven Pile Footings," Structure Notes, No. 22, California Department of Transportation (Caltrans), Division of Structures, March 1991.

(4) Lam, P. I. and Martin, G. R., "Seismic Design of Highway Bridge Foundations," Report No. FHWA/RD-86/101, Federal Highway Administration, Office of Engineering and Highway Operations, June 1986.